

Investigating the Annual Behaviour of Submicron Secondary Inorganic and Organic Aerosols in London

D. E. Young^{1,*}, J. D. Allan^{1,2}, P. I. Williams^{1,2}, D. C. Green³, M. J. Flynn¹, R. M. Harrison^{4,5}, J. Yin⁴, M. W. Gallagher¹, and H. Coe¹

[1]{School of Earth, Atmospheric and Environmental Sciences, University of Manchester, Oxford Road, Manchester, M13 9PL, UK}

[2]{National Centre for Atmospheric Science, University of Manchester, Oxford Road, Manchester, M13 9PL, UK}

[3]{School of Biomedical and Health Sciences, King's College London, London, UK}

[4]{School of Geography, Earth and Environmental Sciences, University of Birmingham, Edgbaston, Birmingham, B15 2TT, United Kingdom}

[5]{Department of Environmental Sciences / Center of Excellence in Environmental Studies, King Abdulaziz University, Jeddah, 21589, Saudi Arabia}

[*]{Now at Department of Environmental Toxicology, University of California, Davis, CA, 95616, USA}

Correspondence to: H. Coe (hugh.coe@manchester.ac.uk)

Abstract

For the first time, the behaviour of non-refractory inorganic and organic submicron particulate through an entire annual cycle is investigated using measurements from an Aerodyne compact time-of-flight aerosol mass spectrometer (cToF-AMS) located at a UK urban background site in North Kensington, London. We show secondary aerosols account for a significant fraction of the submicron aerosol burden and that high concentration events are governed by different factors depending on season. Furthermore, we demonstrate that on an annual basis there is no variability in the extent of secondary organic aerosol (SOA) oxidation, as defined by the oxygen content, irrespective of amount. This result is surprising

1 given the changes in precursor emissions and contributions as well as photochemical activity
2 throughout the year; however it may make the characterisation of SOA in urban
3 environments more straightforward than previously supposed.

4 Organic species, nitrate, sulphate, ammonium, and chloride were measured during 2012 with
5 average concentrations (\pm one standard deviation) of 4.32 (\pm 4.42), 2.74 (\pm 5.00), 1.39 (\pm
6 1.34), 1.30 (\pm 1.52) and 0.15 (\pm 0.24) $\mu\text{g m}^{-3}$, contributing 43%, 28%, 14%, 13% and 2% to
7 the total non-refractory submicron mass (NR-PM₁), respectively. Components of the organic
8 aerosol fraction are determined using positive matrix factorisation (PMF) where five factors
9 are identified and attributed as hydrocarbon-like OA (HOA), cooking OA (COA), solid fuel
10 OA (SFOA), type 1 oxygenated OA (OOA1), and type 2 oxygenated OA (OOA2). OOA1
11 and OOA2 represent more and less oxygenated OA with average concentrations of 1.27 (\pm
12 1.49) and 0.14 (\pm 0.29) $\mu\text{g m}^{-3}$, respectively, where OOA1 dominates the SOA fraction
13 (90%).

14 Diurnal, monthly, and seasonal trends are observed in all organic and inorganic species, due
15 to meteorological conditions, specific nature of the aerosols, and availability of precursors.
16 Regional and transboundary pollution as well as other individual pollution events influence
17 London's total submicron aerosol burden. High concentrations of non-refractory submicron
18 aerosols in London are governed by particulate emissions in winter, especially nitrate and
19 SFOA, whereas SOA formation drives the high concentrations during the summer. The
20 findings from this work could have significant implications for modelling of urban air
21 pollution as well as for the effects of atmospheric aerosols on health and climate.

22

23 **1 Introduction**

24 Atmospheric aerosols have adverse effects on human health (Pope and Dockery, 2006), air
25 quality (AQEG, 2012), visibility (Watson, 2002), and climate (Boucher et al., 2013).
26 Pollution abatement is therefore important, especially in cities, when three-quarters of
27 Europe's population currently live in urban areas, a number that is expected to increase to
28 80% by 2020 (EEA, 2010). Regulations on air quality are based on PM₁₀ and, more recently,
29 PM_{2.5} (particulate matter with aerodynamic diameters less than 10 μm and 2.5 μm
30 respectively, European Union, 2008). A recent study (Aphekom Summary Report, 2011)
31 reported that life expectancy in London could increase by 2.5 months for persons 30 years of
32 age and older if average annual PM_{2.5} concentrations were decreased in line with the World

1 Health Organization's Air quality guidelines to $10 \mu\text{g m}^{-3}$ (WHO, 2005). PM_{10} (particulate
2 matter with an aerodynamic diameter less than $10 \mu\text{m}$) is beginning to receive greater attention
3 from the air quality community as they are associated with adverse health effects due to the
4 depth within the lungs to which these particles can penetrate and can then enter the blood
5 stream, and cause damage to other parts of the body (Oberdörster et al., 2005).

6 Primary and secondary aerosols have both natural and anthropogenic sources (Seinfeld and
7 Pandis, 2006), resulting in their diverse chemical composition, size, and concentration
8 (Pöschl, 2005). In urban areas, primary aerosols from transport, cooking, and solid fuel
9 burning are of great significance (Allan et al., 2010), particularly in the winter when
10 meteorological conditions are such that their concentrations are elevated resulting in pollution
11 events (Zhang et al., 2007; Huang et al., 2014). In addition, transported air masses frequently
12 influence the UK's atmosphere (Abdalmogith and Harrison, 2005) including polluted air
13 masses from continental Europe and cleaner westerly conditions. Transported pollution
14 typically comprises secondary aerosols, with season having a strong influence on the
15 chemical composition and concentration (Charron et al., 2007). Previous studies highlight the
16 variability in the contribution of both secondary inorganic and organic aerosol (SIA and
17 SOA, respectively) to the total mass depending on location (Jimenez et al., 2009).
18 Furthermore, chemical composition varies with location due to a combination of local and
19 regional aerosol sources as well as daily and seasonal meteorological conditions.

20 The precursors and formation processes of SIA are relatively well understood, particularly as
21 anthropogenic emissions dominate although concentrations are significantly influenced by
22 regional and transboundary pollution. For example, Abdalmogith and Harrison (2006)
23 estimated that between 2002 and 2004, 88% of nitrate and 92% of sulphate in central London
24 originated from the regional background. Due to the non-linear response of SIA
25 concentrations from reductions in precursor emissions, the impacts on formation from
26 changes in emissions are uncertain (AQEG, 2012). In contrast, the complexity of SOA
27 precursors, including the range of atmospheric processing they can undergo, lifetime, and
28 temporal and spatial variability presents a major challenge to understanding and
29 characterising SOA and its formation (Goldstein and Galbally, 2007). Additional variability
30 of SOA sources and formation results from the long distances over which SOA precursors
31 and the resulting aerosols can be transported as well as dependency on meteorological
32 conditions (Martin et al., 2011). Furthermore, SOA evolves in the atmosphere with properties

1 changing with age (Ng et al., 2010) meaning our ability to quantify and predict SOA remains
2 limited.

3 The Aerodyne Aerosol Mass Spectrometer (AMS) measures size-resolved chemical
4 composition of non-refractory submicron particulates with high time resolution (Jayne et al.,
5 2000; Canagaratna et al., 2007). The AMS has demonstrated its versatility in a range of
6 environments across the world (Zhang et al., 2007) and has been used to successfully
7 investigate SOA behaviour (e.g. Jimenez et al., 2009; Heald et al., 2010; Ng et al., 2010;
8 Kroll et al., 2011). However, despite its widespread use in such process studies, the
9 instrument is infrequently used for long-term characterisation of aerosols. The related aerosol
10 chemical speciation monitor (ACSM, Ng et al., 2011a), however, is routinely used for long-
11 term measurements of aerosol chemical composition. Here we present a year-long UK urban
12 background data set collected with a compact time-of-flight AMS (cToF-AMS) including
13 results of positive matrix factorisation (PMF) analysis, which is the first time the AMS has
14 been used in this way in an urban environment. The temporal trends and contributions of
15 urban aerosols to PM_{10} are evaluated and their sources are investigated. In this paper we will
16 focus on the secondary aerosols; though primary organic aerosol sources are identified in this
17 paper, the behaviour of primary aerosols from these sources will be discussed in subsequent
18 publications.

19 In Section 2 of the paper, the experimental site, instrumentation, and analysis methods
20 utilised in this study are described. In Section 3, an overview of the bulk non-refractory PM_{10}
21 (NR- PM_{10}) components including average mass, diurnal profiles, and seasonality is presented
22 along with a discussion on the factors governing concentrations and temporal trends. In
23 Section 4, the components of the organic fraction are investigated using receptor modelling.
24 In Section 4.3, we investigate two covarying factors derived from PMF analysis, with the
25 method used to estimate the concentrations of the two factors described in Section 4.4. In
26 Section 5, the organic components are identified and the results from the previous sections
27 are used to probe the behaviour of urban SOA including temporal trends (Section 5.1) and
28 state of oxidation (Section 5.2). In Section 6, the factors governing pollution events across the
29 year, as well as winter and summer, are assessed through identification of the dominant
30 components of the high concentration events. Finally, Section 7 summarises the conclusions
31 from this study on secondary aerosols in London.

32

1 **2 Experimental**

2 **2.1 Site and instrumentation**

3 The measurements for this study were conducted as part of the Natural Environment
4 Research Council (NERC) funded Clean Air for London (ClearLo) Project
5 (www.clearflo.ac.uk), a large, multi-institutional collaborative scientific project based in the
6 UK. A suite of state-of-the-art instrumentation, measuring aerosols, gases, radicals and
7 meteorological parameters was deployed for two major intensive observation periods (IOPs)
8 during 2012, with long-term continuous measurements conducted between 2011 and 2013.
9 Measurements were conducted at the ClearLo urban background site in the grounds of a
10 school in North Kensington (51.521055 N, 0.213432 W), where a permanent Department for
11 Environment, Food and Rural Affairs (DEFRA) Automated Urban and Rural Network
12 (AURN, <http://uk-air.defra.gov.uk/networks/network-info?view=aur>) monitoring station is
13 located. A background site is defined by DEFRA as being located such that its pollution level
14 is not influenced significantly by any single source or street, but rather by the integrated
15 contribution from all sources upwind of the station” and “be representative for several square
16 kilometres”. Situated in a residential area 7 km to the west of Central London, the sampling
17 site is not influenced by heavily trafficked roads and is representative of background air
18 quality (Bigi and Harrison, 2010). Along with the school buildings, a car park and a relatively
19 large playing field are also located at the site with several large trees both on site and lining
20 the surrounding pavements. Further details on the ClearLo experimental campaigns and
21 locations are described in Bohnenstengel et al. (2014).

22 Aerosol chemical composition was measured by the cToF-AMS for a full calendar year (11
23 January 2012 – 23 January 2013) and by the high-resolution time-of-flight AMS (HR-ToF-
24 AMS) during the two IOPs, which were conducted in the winter (January – February) and
25 summer (July – August) of 2012. The cToF-AMS sampled through a PM_{2.5} inlet, with a
26 bypass flow of 16 l min⁻¹ and split using an asymmetric Y-piece. The HR-ToF-AMS was
27 located in a shipping container containing several other aerosol instruments, where aerosols
28 were sub-sampled from a sampling stack with a flow of 30 l min⁻¹ via a 3.5 µm cut-off
29 cyclone.

30 Both AMS instruments operated in the standard configuration and took mass spectra (MS)
31 and particle time of flight (pToF) data. An overview of the AMS can be found in Canagaratna
32 et al. (2007) and detailed descriptions of both the cToF-AMS and HR-ToF-AMS can be

1 found in Drewnick et al. (2005) and DeCarlo et al. (2006) respectively. The instrument
2 operation and data analysis procedures pertinent to this study have been described elsewhere
3 (e.g. Allan et al., 2010). The HR-ToF-AMS operated in both ‘V’ and ‘W’ ion path modes,
4 offering high sensitivity but low mass resolution, and low sensitivity but high mass
5 resolution, respectively. Only the V mode ambient data are analysed further here due to their
6 better signal-to-noise ratio. The time-resolution of the cToF-AMS was 5 minutes throughout
7 the measurement period. As the HR-ToF-AMS sampled in an alternating sequence with other
8 black carbon and aerosol volatility measurements using a thermodenuder (Huffman et al.,
9 2008) in the winter, 5-minute averaged ambient data in V mode were only obtained every 30
10 minutes. In the summer, there were no volatility measurements so average data were obtained
11 every 12 minutes. Both instruments were calibrated using 350nm mono-disperse ammonium
12 nitrate particles approximately once a month for the cToF-AMS and weekly during the IOPs
13 for the HR-ToF-AMS. Ammonium sulphate calibrations were also performed where possible.
14 The heater bias of the cToF-AMS was tuned to minimise the signal from surface ionised
15 potassium and the filament was run at a lower value than usual in order to prolong the life of
16 the multi-channel plate (MCP). This configuration results in a reduced signal, which in turn
17 reduces the signal-to-noise ratio (Allan et al., 2003).

18 **2.2 Analysis and quality control of AMS data**

19 CToF-AMS data were analysed within Igor Pro (Wavemetrics) using the standard TOF-AMS
20 analysis toolkit software package, SQUIRREL (SeQUential Igor data RetRIeval) v1.53. The
21 HR-ToF-AMS data were analysed using SQUIRREL v1.52J and PIKA v1.11J (Sueper,
22 2008). An average ionisation efficiency (IE) determined from all calibrations was applied to
23 the full data set. Relative ionisation efficiencies (RIEs) of ammonium, nitrate, and sulphate
24 were estimated based on the molar ratios of each species from the ammonium nitrate
25 calibrations (see Table S1 in the Supplementary Information for the ammonium and sulphate
26 RIE values for the cToF-AMS and HR-ToF-AMS). These were compared to particulate
27 sulphate measurements from the URG-9000B Ambient Ion Monitor (AIM) from North
28 Kensington (AURN and Particle Numbers and Concentrations Network, [http://uk-
29 air.defra.gov.uk/networks/network-info?view=particle](http://uk-air.defra.gov.uk/networks/network-info?view=particle)) where available (Fig. S1) and indicated
30 that the default RIE of sulphate of 1.2 may not be appropriate for either instrument. As a
31 sulphate calibration was not performed on the HR-ToF-AMS during the winter IOP the RIE
32 was ambiguous, so concentrations were based on those reported by the cToF-AMS, which

1 was calibrated later during the campaign (see Section 2.1 in Supplementary Information for a
2 comparison of the concentrations between the two instruments for the winter IOP and Section
3 2.2 for the summer IOP). This approach, as opposed to using the default RIE of 1.2, was
4 deemed valid as it resulted in a more consistent volume concentration comparison with that
5 derived from a differential mobility particle sizer (DMPS) from the winter IOP (Fig. S2)
6 where the volume concentration was estimated using the densities reported by Cross et al.
7 (2007). A time and composition dependent collection efficiency (CE) was applied to the data
8 based on the algorithm by Middlebrook et al. (2012). This was also validated for both AMSs
9 by comparing the volume concentration with that derived from the DMPS measurements
10 from the winter IOP (Figs. S2a and d).

11 Inspection of the data revealed step changes in cToF-AMS mass concentrations that
12 coincided with changes in the flowrate, which were mostly due to partial blockages in the
13 pinhole (see Section 1.2 in the Supplementary Information). In each case, the pinhole was
14 either manually cleaned (through sonication in deionised water) or the flow returned to its
15 average rate of 1.3 cc/sec without intervention. Data were removed if clear mass changes
16 were observed, with distinct start and end points (e.g. 2 June 2012, Fig. S3b). Other data were
17 flagged as suspect if the flow was significantly different from its normal rate (less than 1.2
18 cc/sec) but there were no distinct step changes in mass e.g. 4 September 2012 (Fig. S3c). The
19 final data set comprised 95% data that had not been removed or flagged as suspect.

20 **2.3 Levoglucosan measurements**

21 24-hour PM_{2.5} samples were collected on quartz fibre filters (Whatman QM-A) at NK during
22 the winter 2012 ClearLo campaign using a high volume Digitel DHA-80 sampler at a flow
23 of 500 l/min. These samples were analysed for wood smoke marker levoglucosan using a
24 slightly modified version of the method of Yin et al. (2010) and Wagener et al. (2012). In
25 brief, one portion of the Digitel filter sample was spiked with an internal standard (IS),
26 methyl-beta-D-xylopyranoside (from Sigma-Aldrich Ltd) and extracted with
27 dichloromethane and methanol under mild sonication at room temperature. The combined
28 extract was filtered and concentrated down to 50 µl. One aliquot of the extract was
29 evaporated to near dryness and derivatised by addition of N,O-
30 bis(trimethylsilyl)trifluoroacetamide plus 1% trimethylchlorosilane (BSTFA + 1% TMCS)
31 and pyridine at 70°C for 1h, and finally cooled in a desiccator. Quantification was based on
32 the IS and a six point authentic standard calibration curve, using the selected ion monitoring

1 (SIM) mode on an Agilent GC-MS instrument. The ions monitored were 204 and 217 for the
2 IS and 204, 217 and 333 for levoglucosan.

3

4 **3 Results**

5 The daily averaged time series of NR-PM₁ species, their diurnal patterns, and monthly
6 average contributions to total submicron mass are shown in Fig. 1. On average, PM₁
7 composition is dominated by the organic fraction (Org, 44%, Fig. 2) with the remainder of
8 the total mass comprising SIA species. Nitrate (NO₃) is the largest SIA component,
9 comprising 28% of the total mass. Sulphate (SO₄) and ammonium (NH₄) contribute 14% and
10 13% respectively with a small contribution from non-refractory chloride (Chl, 1%). The
11 contribution of each species to the total mass varies with time; organics dominate in summer
12 and inorganics dominate in winter, with nitrate contributing up to 45% of the total mass in
13 spring (Fig. 1c).

14 Organic species constituted, on average, just under half of the non-refractory submicron mass
15 as measured by the AMS in 2012 (44%, Fig. 2), with a mean annual concentration (\pm one
16 standard deviation) of 4.32 (\pm 4.42) $\mu\text{g m}^{-3}$. During the year, concentrations at times
17 increased up to, and over, an order of magnitude greater than this value with a maximum 5
18 minute concentration of 230 $\mu\text{g m}^{-3}$, observed on 18 February. This is likely a locally sourced
19 event lasting approximately 6 hours as the maximum daily concentration was 16.97 $\mu\text{g m}^{-3}$,
20 observed on 25 July (Fig. 1a). The mean organic concentrations and diurnal patterns exhibit
21 little seasonality (Figs. S6a and b, respectively); a large evening peak is observed in all
22 diurnal profiles but the number of peaks and their timing during the day vary slightly with
23 season. Although the total mass of organic species exhibits little seasonality, the organic
24 fraction of total PM₁ varies with season, being largest in summer and autumn.

25 The average annual PM₁ nitrate concentration was 2.74 (\pm 5.00) $\mu\text{g m}^{-3}$ with several high
26 concentration episodes occurring throughout the year (Fig. 1a). Peak events occurred mainly
27 during the winter and spring, with a maximum 5 minute concentration of 48.35 $\mu\text{g m}^{-3}$
28 measured on 23 March. Increases in the concentrations of all species are also observed
29 during these high nitrate events. Averaged across the year, nitrate exhibits a pronounced
30 diurnal pattern with an overnight increase in mass, peaking at 08:00 UTC, with a daytime
31 minimum at 16:00 UTC (Fig. 1b). The overall shape of the diurnal pattern varies little with
32 season although it becomes less pronounced in summer and autumn (Fig. S7b). In contrast,

1 the total nitrate mass varies significantly with season (Fig. S7a), where the greatest
2 concentrations are observed during the spring, which is also when the diurnal pattern is most
3 pronounced due to a large range of concentrations. The lowest concentrations and smallest
4 diurnal range occur during the summer months.

5 Submicron sulphate represents approximately 25% of the inorganic fraction, with a mean
6 concentration of $1.39 (\pm 1.34) \mu\text{g m}^{-3}$. The maximum 5 min sulphate concentration measured
7 in 2012 was $12.75 \mu\text{g m}^{-3}$ which occurred on 2 May. In general, increases in sulphate mass
8 are coincident with increases in concentration of other AMS measured species. In contrast to
9 nitrate, sulphate exhibits little seasonality although it dominates SIA mass in summer, with
10 higher mean concentrations occurring in spring and summer compared to autumn and winter
11 (Fig. S8a). Furthermore, sulphate exhibits little diurnal variation for each season as well as
12 for the whole year (Figs. S8b and 1b).

13 Almost a quarter of the inorganic mass fraction is comprised of ammonium, with a mean
14 concentration of $1.30 (\pm 1.52) \mu\text{g m}^{-3}$. Averaged across the year, ammonium exhibits a weak
15 diurnal profile (Fig. 1b). However, this pattern varies with season, with a peak in
16 concentration between 08:00 and 10:00 UTC in all but the summer months (Fig. S9b). The
17 most pronounced diurnal variability occurs in spring, which is also when there is the greatest
18 seasonal mass (Fig. S9a) and maximum concentration of the year ($14.23 \mu\text{g m}^{-3}$). The aerosol
19 was found to be neutral throughout the year as the balance between inorganic cationic and
20 anionic charge was maintained.

21 As the AMS does not detect chloride salts such as sodium chloride, the chloride measured
22 here is primarily ammonium chloride. Although this represents a very small fraction of SIA,
23 with an average concentration of $0.15 (\pm 0.24) \mu\text{g m}^{-3}$, some seasonal differences are
24 apparent. Chloride exhibits a weak diurnal pattern with slightly higher concentrations at night
25 compared to during the day (Fig. 1b), which changes with season (Fig. S10b). The highest
26 chloride concentrations are in the winter with comparatively low concentrations in the
27 summer (Fig. S10a).

28 **3.1 Behaviour of bulk PM₁ components**

29 **3.1.1 Organic aerosols**

30 Weak seasonality of organic aerosols in Paris has been previously suggested (e.g. Freutel et
31 al., 2013) and observed in organic carbon (OC) measurements in Birmingham (Harrison and

1 Yin, 2008). The lack of seasonality arises because of the balance of sources that govern the
2 total concentration of organic species differently during each season (Zhang et al., 2007)
3 rather than the constancy of any particular source. As well as differences in sources with
4 season, increased organic concentrations in winter are due to low temperatures and reduced
5 atmospheric mixing, whereas in summer similar concentrations are due to increased
6 photochemistry (Martin et al., 2011). In contrast to absolute mass, there are differences in the
7 organic fraction of total PM₁ with season, which have been observed in Paris (Crippa et al.,
8 2013a; Freutel et al., 2013), Tokyo (Takegawa et al., 2006), and Zurich (Lanz et al., 2007),
9 and can be attributed to seasonal differences in concentrations of other species such as nitrate.
10 Consistent with previous observations, organics in London exhibit little seasonality both in
11 terms of mass and diurnal profile. Any variations in diurnal pattern across the year are due to
12 both mixing layer height dynamics and the nature of the dominant source. The components of
13 the organic aerosol fraction are discussed in more detail in Section 4.

14 **3.1.2 Nitrate**

15 The annual cycle of nitrate mass is significantly influenced by season (Martin et al., 2011),
16 driven by emissions of ammonia, which typically peak in the spring (Schaap et al., 2004), as
17 well as temperature and relative humidity (RH), which both control nitrate partitioning
18 (Stelson and Seinfeld, 1982). The diurnal pattern of nitrate in urban locations (e.g. Cork,
19 Dall'Osto et al., 2013; Paris, Freutel et al., 2013) is also largely governed by the semi-volatile
20 behaviour of ammonium nitrate. However, nitrate formation also strongly depends on
21 availability of precursor gases (Ansari and Pandis, 1998) such as nitrogen oxides (NO_x) and,
22 in particular, ammonia, as emissions in urban environments are small compared to NO_x
23 (NAEI, 2013). Although some non-agricultural sources of ammonia are known (Sutton et al.,
24 2000), their strengths and trends are not well understood. Pollution from continental Europe
25 has also been identified as an important contributor to particulate concentrations in many
26 regions (e.g. Manchester, Martin et al., 2011; Paris, Freutel et al., 2013) with the highest
27 nitrate concentrations occurring over North West Europe during pollution episodes (Morgan
28 et al., 2010).

29 Consistent with previous UK measurements (Harrison and Yin, 2008; AQEG, 2012), the
30 highest concentrations in this study occurred in spring. Although more pronounced in winter
31 and spring, the overall shape of the diurnal profile does not change with season, indicating
32 the strong semi-volatile behaviour of nitrate. Also consistent with previous studies (e.g.

1 Abdalmogith and Harrison, 2005), increased nitrate concentrations occur in air masses
2 influenced by continental North-Western Europe, indicating the importance of transboundary
3 pollution. Nitrate concentrations are therefore governed by a combination of season, ambient
4 conditions, availability of precursor emissions, and air mass trajectory rather than any one
5 factor. Consequently, it was not possible to establish simple metrics that could be used to
6 predict nitrate concentrations, highlighting the need for detailed modelling of aerosol
7 chemistry and thermodynamics to accurately predict nitrate concentrations.

8 **3.1.3 Sulphate**

9 Sulphate concentrations have been decreasing at both urban and rural UK locations for at
10 least the last 10 years (as summarised in Table 1) due to decreasing SO₂ emissions (Monks et
11 al., 2009). However, sulphate concentrations respond non-linearly to reductions in SO₂
12 emissions (Megaritis et al., 2013). The mean sulphate concentration (1.39 µg m⁻³) measured
13 by the AMS in 2012 is comparable to the non-sea salt sulphate (1.21 µg m⁻³) calculated from
14 AIM measurements also at North Kensington. The 2012 AMS measurements are therefore
15 consistent with the trend of decreasing sulphate concentrations observed at sites at North
16 Kensington and Harwell. Similar to the findings of Harrison et al. (2012) and Abdalmogith
17 and Harrison (2006), sulphate exhibits little seasonality and diurnal variation thus
18 emphasising the importance of regional pollution.

19 **3.1.4 Ammonium**

20 Changes in the diurnal profile and total mass of ammonium with season are very similar to
21 those of nitrate and, to a lesser extent, sulphate (Morgan et al., 2009; Bressi et al., 2013). The
22 springtime peak in concentrations is governed by the greater availability of ammonia and
23 favourable meteorological conditions.

24 **3.1.5 Chloride (non-refractory)**

25 The seasonal variation and diurnal pattern of chloride is attributed to the semi-volatile nature
26 of ammonium chloride as well as planetary boundary layer dynamics where low
27 concentrations are expected during the summer due to increased mixing depth. The
28 availability of ammonia will also govern the concentration of chloride. In addition, increased
29 chloride concentrations in the winter could be attributable to increased coal combustion
30 during this period (Sun et al., 2013).

31

4 Positive matrix factorisation analysis

To investigate the components and temporal trends of the organic fraction, positive matrix factorization (PMF) (Paatero and Tapper, 1994; Lanz et al., 2007) was applied to the organic matrix from the year-long cToF-AMS data set, which is the first time PMF has been applied to a data set of this duration from an urban environment. Separating long-term data into seasons before performing factorisation analysis may be used to reduce seasonal phenomena affecting the retrieved factors, such as minimising the influence of variations in photochemistry and also to address known PMF limitations such as mixing between factors. However, splitting the data into seasons is subjective, resulting in a bias of the retrieved factors and loss of information on annual trends of potential OA components.

Identification of key organic components can also be achieved by using the related multilinear engine ME-2, for which a protocol for the AMS is currently available (Canonaco et al., 2013) and has been found to produce more representative results in some circumstances (e.g. Lanz et al., 2008), particularly when temporal co-variation of factors arises. However, a priori knowledge by way of factor profiles and/or time series is required to utilise ME-2, so in principle it is preferable to obtain a factorisation without a priori assumption, which is achieved in this study by way of unconstrained PMF analysis. Furthermore, several of the factorisation problems that ME-2 overcomes when applied to data from the ACSM (Ng et al., 2011a) compared to the AMS are related to the fact that the ACSM has much lower signal-to-noise ratio (approximately by a factor of 40). We present the results from PMF analysis here to compare with earlier work and as a first stage in any further analysis. Furthermore, as we will show in the data presented, temporal co-variation of factors can be overcome by careful scrutiny of the data as well as from the use and support of associated measurements such as from the HR-ToF-AMS.

4.1 Data preparation

PMF was performed on the organic data matrix for the year-long data set from the cToF-AMS and for the winter and summer periods when the HR-ToF-AMS was operating. The data preparation for all three data sets followed the recommended procedures as described by Ulbrich et al. (2009). However, for the final PMF solution, the summer period was removed from the cToF-AMS data set, as the mass spectrometer was mistakenly re-tuned for this period, which caused problems for the factorisation. The changes in the instrumental settings were evident in the data as the concentrations of several of the factors derived from PMF

1 analysis increased simultaneously with a step change in the heater bias. However, due to the
2 nature of the affected factors and the timing of the instrumental changes, it was not possible
3 to calculate a reliable scaling factor to apply to the data from this period. The reader is
4 directed to Sects. 4.1 and 4.2 in the Supplement for more details regarding the data pre-
5 treatment and quality assurance, including the identification and removal of problematic data
6 around the summer IOP. In addition to the standard methods, isotopes were not included in
7 the HR-ToF-AMS organic matrix. The peaks at m/z 30 and 46 were removed from the
8 matrix, as they were not deemed to have been successfully retrieved using PIKA. APES light
9 v1.05 (Sueper, 2008) was used for the elemental analysis of the HR-PMF factors.

10 **4.2 Factorisation results**

11 A 5-factor solution to the PMF analysis was shown to be optimum for the cToF-AMS data
12 set. The details of the choice of factors and solution criteria can be found in the
13 Supplementary Information, Section 4.3. The reader is referred to Section 5 in the
14 Supplementary Information for the HR-ToF-AMS PMF (HR-PMF) solution criteria, where 5-
15 factor solutions were chosen for both the winter and summer IOPs (Sections 5.1 and 5.2 in
16 the Supplementary Information, respectively). The cToF-AMS PMF (cToF-PMF) solution
17 criteria are briefly outlined here.

18 The 5-factor solution resulted in a better separation of the mass spectral profiles compared to
19 the 4-factor solution, with improvements to diagnostics, such as Q/Q_{expected} , used to assess the
20 quality and suitability of a solution set. The 6-factor solution was discarded due to the
21 similarity of several factors (spectra and time series). The 7-factor solution was also
22 discarded due to its significant dependency on the initialisation seed (unlike the solutions
23 with fewer factors) as well as the production of a factor that did not appear physically
24 meaningful. The 'fPeak' parameter was used to explore the rotational ambiguity of the 5-
25 factor solution with the most central solution (fPeak=0) chosen for further analysis.
26 Additional measurements were used to validate the chosen solution and for attribution of the
27 factors.

28 Three of the five PMF factors were clearly identifiable: hydrocarbon-like OA (HOA),
29 cooking OA (COA), and type 1 oxygenated OA (OOA1). As the remaining two factors
30 (labelled here as SFOA_{PMF} and OOA2_{PMF}) exhibited similar temporal features, notably the
31 diurnal pattern (Fig. 3) with an evening peak in concentration, they are investigated and
32 addressed in detail in the following sections.

1 4.3 Identifying PMF limitations

2 The similarity of the diurnal patterns of $SFOA_{PMF}$ and $OOA2_{PMF}$ is likely due to the nature of
3 the aerosols where $SFOA_{PMF}$ is likely emitted from domestic space heating, an activity that
4 occurs in the evening. $OOA2_{PMF}$ is typically thought to be semi-volatile oxygenated OA (SV-
5 OOA) and will preferentially partition to the particle phase when temperatures are low and
6 RH is high, again most likely in the evening. Conversely, the temporal co-variation of the
7 PMF solution could result in partial mixing of these two factors (Crippa et al., 2013b) leading
8 to the identification of an OOA2-BBOA factor (Crippa et al., 2013a). However, a clearer
9 separation of such factors was obtained through combined AMS and Proton Transfer
10 Reaction Mass Spectrometry (PTR-MS) PMF analysis (Crippa et al., 2013b).

11 The mass spectral profiles and time series of the cToF-PMF factors are compared to the
12 winter IOP HR-PMF factors, as factor retrieval from HR-ToF-AMS data is more robust with
13 significantly reduced rotational ambiguity and improved separation of factors as individual
14 ion signals at the same nominal mass-to-charge ratio (m/z) are included (see Section 6 in the
15 Supplementary Information for comparisons of the mass spectra and time series from the
16 winter and summer IOPs where available). In general, there is good correlation between most
17 factors from the two instruments (Pearson's r of 0.69-0.90, Table 2). However, the
18 concentration of the combined SFOA factors from the winter HR-PMF data set is
19 approximately double that of the cToF-PMF $SFOA_{PMF}$ factor. A near equal concentration of
20 SFOA from both AMSs is achieved when the cToF-PMF $OOA2_{PMF}$ is combined with the
21 $SFOA_{PMF}$ and correlated with the sum of HR-PMF SFOA factors. This suggests that most of
22 the $SFOA_{PMF}$ mass measured by the cToF-AMS is being assigned to $OOA2_{PMF}$ in PMF; the
23 total SFOA mass could therefore be up to a factor of two greater than previously estimated.

24 If SFOA represents all of levoglucosan and other similar species, we might expect good
25 correlation between SFOA and levoglucosan to exist. As org60 (the organic fraction at m/z
26 60) has contributions from fatty acids arising from cooking POA emissions (Mohr et al.,
27 2009) and carboxylic acids from SOA (e.g. DeCarlo et al., 2008), it is not expected that org60
28 and levoglucosan would correlate exactly when compared. $SFOA_{PMF}$ and
29 $SFOA_{PMF}+OOA2_{PMF}$ are compared to 24-hour filter measurements of levoglucosan from the
30 winter IOP. $SFOA_{PMF}+OOA2_{PMF}$ correlates better with levoglucosan than $SFOA_{PMF}$ on its
31 own (Pearson's r of 0.74 and 0.71 respectively), suggesting that some of the additional
32 variance is carried by a levoglucosan contribution to $OOA2_{PMF}$. Furthermore, org60
33 correlates slightly better with levoglucosan than $SFOA_{PMF}$ (Pearson's $r = 0.73$), again

1 suggesting that $SFOA_{PMF}$ is not capturing all the variability of levoglucosan. However, it is
2 unlikely that this is the full explanation as the m/z 60 signal of $OOA2_{PMF}$ is relatively small.
3 The possibility that $OOA2_{PMF}$ could be an overlap of what is $OOA1$ in the summer and an
4 aged SFOA in the winter has been explored but correlations between $OOA2_{PMF}$ and nitrate
5 suggest that this is not likely to be the case.

6 This is not to suggest that all $OOA2$ factors contain some contribution of SFOA. However, if
7 SFOA is convolved with $OOA2$, as is the case in this study, it is possible to estimate the
8 proportion of SFOA convolved with $OOA2$ with the support of additional measurements. In
9 this study we have shown that comparisons of measurements from the two AMSs highlighted
10 a large difference in SFOA concentrations, which was further supported by levoglucosan
11 measurements and those from the cToF-AMS itself such as $org60$. Improved separation of
12 OA factors may be achieved in the future, particularly in the absence of supporting
13 measurements, from the application of ME-2 to similar data sets such as those from the
14 ACSM. However, further work is therefore required to better resolve the issues arising from
15 PMF analysis regarding the separation of OA in to its primary and secondary constituents,
16 particularly for long-term data sets.

17 **4.4 Estimating concentrations of convolved factors**

18 We infer from the correlations discussed in Section 4.3 that nearly all the $SFOA_{PMF}$ is
19 assigned to $OOA2_{PMF}$ during the winter IOP, where the proportion of $SFOA_{PMF}$ that is
20 convolved with OOA_{PMF} can be determined using the relationship between $SFOA_{PMF}$ and
21 OOA_{PMF} from the winter. Both factors have similar, strong diurnal profiles, the effect of
22 which is reduced by using daily averages of each factor in the following equation:

$$23 \quad OOA2_{PMF} = a.SFOA_{PMF} + OOA2_{noSF} \quad (1)$$

24 where a is the gradient of an orthogonal distance regression fit, equal to 0.86, and $OOA2_{noSF}$
25 is the intercept which indicates the amount of $OOA2_{PMF}$ without a solid fuel signature. The
26 remainder is the $SFOA_{PMF}$ assigned to $OOA2_{PMF}$ during the PMF analysis and is estimated
27 based on the gradient of the fit. The SFOA and $OOA2$ concentrations, $SFOA_{mod}$ and
28 $OOA2_{mod}$ respectively, can therefore be calculated using the following equations:

$$29 \quad SFOA_{mod} = SFOA_{PMF} + (a.SFOA_{PMF}) \quad (2)$$

$$30 \quad OOA2_{mod} = OOA2_{PMF} - (a.SFOA_{PMF}) \quad (3)$$

1 where $OOA2_{mod}$ in equation 3 is equivalent to $OOA2_{noSF}$ in equation 1. The relationship
2 based on the winter correlation does not hold true for the whole year and so the annual
3 estimations are improved by using the relationship derived between the daily averages of
4 $OOA2_{PMF}$ and $SFOA_{PMF}$ from December 2012-January 2013, where a is equal to 0.52.
5 However, instrument maintenance (changes in instrument tuning during the summer and
6 change of the MCP in April) will likely add some variation to these estimates. Therefore, the
7 concentrations up until the summer period are estimated using the relationship from the 2012-
8 January 2013 relationship. The estimated concentrations of $OOA2_{mod}$ and $SFOA_{mod}$ are used
9 for further analyses. Figure 4 shows the retrieved $OOA2_{mod}$ is dominated by noise, with an
10 average $OOA2_{mod}$ concentration of $0.12 \mu\text{g m}^{-3}$ and standard deviation of $0.46 \mu\text{g m}^{-3}$ during
11 the winter IOP. The standard deviation provides a measure of uncertainty in our retrieval of
12 $OOA2_{mod}$ and $SFOA_{mod}$ using this approach.
13

14

15 **5 Attribution and contributions of organic components**

16 Attributing the PMF factors to different organic sources and components allows the organic
17 fraction to be split in to primary OA (POA) and secondary OA (SOA) and their contribution
18 to total organic mass to be assessed. The behaviour of urban secondary OA (SOA) can then
19 be investigated. The HOA, COA, and $SFOA_{mod}$ factors identified in the previous sections are
20 grouped as primary OA (POA) and $OOA1$ and $OOA2_{mod}$ are grouped as secondary OA
21 (SOA). The primary fraction has the greatest contribution from $SFOA_{mod}$ 38% (Fig. 2), with
22 smaller contributions from HOA (32%) and COA (30%). The secondary fraction is
23 dominated by $OOA1$ (90%) with only a small contribution from $OOA2_{mod}$ (10%).

24 The greatest contribution of the organic components to total OA mass, which does not
25 include some of the summer period (see Sect. 4.1), is from $OOA1$ (31%), followed by
26 $SFOA_{mod}$ (25%), HOA (21%), and COA (19%). The remainder comprises $OOA2_{mod}$ (4%).
27 During 2012, POA and SOA contributed 65% and 35% to total OA, respectively (Fig. 2).
28 However, the contribution of POA and SOA to total OA changes with season where SOA
29 contributes just over 50% on average during the spring and summer (Fig. 5). The smaller
30 annual contribution from SOA could therefore be partly due to the omitted summer data,
31 where SOA dominates the mass fraction. However, the mean (and standard deviation) ozone
32 mixing ratio was not found to be statistically significantly different between the 5 week

1 period not included in PMF analysis and the whole June, July, and August period, suggesting
2 the data that is included in the analysis is representative of the data that were removed.

3 **5.1 The behaviour of secondary organic aerosol in London background air**

4 The average (\pm one standard deviation) OOA1 concentration observed was $1.27 (\pm 1.49) \mu\text{g}$
5 m^{-3} , with a maximum 5 minute concentration of $19.5 \mu\text{g m}^{-3}$ measured on 24 May 2012.
6 OOA1 does not exhibit a discernible diurnal pattern (Fig. 3), where the only change with
7 season is by way of concentration (Fig. 6a), suggestive of aged aerosol of a regional nature.
8 The peak in concentrations occurs in spring, where the average concentration is more than
9 double that of the autumn and winter and 1.7 times greater than the summer (Fig. 6b). This
10 spring time peak is consistent with secondary OC measurements in Birmingham (Harrison
11 and Yin, 2008).

12 In comparison, the OOA2_{mod} concentration averaged $0.14 (\pm 0.29) \mu\text{g m}^{-3}$ over the year, with
13 maximum daily concentrations occurring in the summer. The seasonal trend of OOA2_{mod} is in
14 keeping with it being secondary in nature with concentrations increasing during the summer
15 (Fig. 6c) when photochemical processes and emissions of biogenic volatile organic
16 compounds (VOCs) (Holmes et al., 2014) are greatest.

17 Several high concentration events lasting 3-8 days are observed in both OOA1 and OOA2_{mod}
18 time series (Fig. 4) such as in May (peaking on 27 May) and to a lesser extent September
19 (peaking on 8-9 September). The event in May is associated mostly with Easterly conditions,
20 likely the result of imported pollution. The September event is associated with a high-
21 pressure system centred just off the SW UK coast with another high pressure system over
22 continental Europe the following day. This resulted in an increase in concentrations in a
23 stagnant air mass with additional imported pollution on the 9 September.

24 **5.2 SOA chemistry and oxidation state**

25 SOA forms in the atmosphere from the gas-phase oxidation of a number of VOCs (e.g.
26 Goldstein and Galbally, 2007), which can be anthropogenic or biogenic in origin. SOA
27 comprises a mixture of organic compounds with differing volatilities (Donahue et al., 2012)
28 which partition between the gas and particle phases. SOA therefore exists across a variety of
29 chemical states thus increasing its chemical complexity. As bulk chemical characterization of
30 aerosols can be obtained from the AMS, several metrics and graphical representations of the
31 data are used to investigate OA. The information gleaned from such metrics can be used to

1 better inform models on SOA characteristics to improve the quantification and prediction of
2 SOA.

3 One such metric for describing and explaining OA evolution in the atmosphere is the f_{44} vs.
4 f_{43} space (Morgan et al., 2010; Ng et al., 2010), where f_{44} and f_{43} are the ratios of the organic
5 signal at m/z 44 and 43 to the total organic signal in the component mass spectrum,
6 respectively. The degree of oxidation is inferred from the f_{44} value and the range of
7 precursors is suggested by the f_{43} values. Other metrics include the use of O:C and H:C ratios
8 in Van Krevelen space which reveals changes in functionality and therefore the likely degree
9 of processing the aerosol has undergone (Heald et al., 2010). Kroll et al. (2011) combined
10 these ratios to derive the oxidation state of carbon and thus describe OA chemistry.
11 Furthermore, the chemical evolution of organic aerosol can be analysed by using the
12 oxidation state along with volatility in the two-dimensional volatility-oxidation space (2D-
13 VBS, Donahue et al., 2012). Despite their differences, these metrics can all be used to
14 describe the evolution of gas-phase organic compounds through to semi-volatile OA and up
15 to the most oxidised OA with low volatility, concluding that atmospheric processing of fresh
16 OA results in similarly aged and highly oxidised OA.

17 To characterise Northern Hemispheric OA and its evolution in the atmosphere, Ng et al.
18 (2010) compiled ambient AMS data from numerous urban and rural ground-based
19 measurement campaigns of varying duration (from a few days up to 5 weeks), occurring
20 during different seasons. Morgan et al. (2010) investigated the organic chemical evolution
21 through various airborne measurement campaigns, tracking individual air masses and
22 crossing a range of European sites during different meteorological conditions. Data from both
23 studies exhibited a range of f_{44} and f_{43} values, reflecting the different photochemical ages and
24 sources. However, all data were found to lie within a very well defined triangular region in f_{44}
25 vs. f_{43} space with OOA1 and OOA2 clustering in discrete regions of the triangular space.
26 This indicated that irrespective of source, atmospheric processes result in the convergence of
27 all ambient OA to chemically similar, highly aged SOA. The most processed OA, with high
28 f_{44} values, in both studies were from rural/remote locations and generally occurred during the
29 summer or during periods of elevated temperatures and greater photochemistry. To further
30 investigate OA evolution and the corresponding changes in chemical composition Ng et al.
31 (2011b) transformed the f_{44} vs. f_{43} triangle into the Van Krevelen diagram (so called VK-
32 triangle). The ambient data from Ng et al. (2010) fall within a narrow range within the VK-

1 triangle whereas two urban data sets from different seasons fall in a narrow linear area (El
2 Haddad et al., 2013).

3 In contrast to the above studies, the measurements in this study are from a single location
4 over the course of a year. In order to investigate trends within the secondary component of
5 OA, the PMF-derived primary components (SFOA_{mod}, HOA, and COA) are subtracted from
6 the total organic aerosol matrix with the remainder assumed to be secondary (hereafter
7 termed SOA_{calc}). Furthermore, to assess the degree of oxidation of the SOA in London the
8 contribution of the primary components to m/z 44 and 43 are subtracted, so the ratio of m/z
9 44:SOA_{calc} to m/z 43:SOA_{calc} can be determined. When plotted in f_{44} vs. f_{43} space, the
10 majority of the data in this study falls within the triangular space defined by Ng et al. (2010)
11 with the average value falling in the OOA1 region (Fig. 7). Along with the range of f_{44}
12 values, correlations with temperature and time can elucidate the extent to which the aerosol is
13 oxidised, where in general, temperatures are elevated and photochemistry is greatest in the
14 summer. Figure 7 illustrates the f_{44} vs. f_{43} space for SOA_{calc} coloured as a function of time
15 (Fig. 7a) and temperature (Fig. 7b). SOA_{calc} exhibits little seasonality, where spring and
16 summer averages have only a slightly higher ratio than autumn and winter, with this variation
17 occurring within a distinct area of the f_{44} vs. f_{43} space. There is also little evidence for a
18 temperature trend (Fig. 7b).

19 OOA1 and OOA2 are thought to represent end members of OA aging from photochemical
20 processing (Jimenez et al., 2009), where OOA1 is more oxygenated and highly aged
21 compared to the fresher and less-photochemically processed OOA2. The f_{44} and f_{43} for the
22 two OOA components identified from PMF analysis in this study, which are fixed factors
23 over the whole one year period, are therefore also plotted within the f_{44} vs. f_{43} space to further
24 constrain the degree of oxidation of what is hypothesised to be London SOA. The two
25 subtypes are found to fall within their respective range of f_{44} values expected for each of the
26 two subtypes, with higher f_{44} and f_{43} for OOA1 than OOA2. Using the relationship between
27 f_{44} and O:C for unit mass resolution data from Aiken et al. (2008), the estimated O:C for the
28 long-term OOA2_{mod} and OOA1 factors are 0.36 and 0.79 respectively. In comparison, for the
29 summer IOP there is only a small difference between the O:C ratio of OOA2 and OOA1
30 (0.44 and 0.52 respectively) obtained from HR-PMF. Here, OOA1 has a much lower ratio
31 compared to other urban studies (e.g. Sun et al., 2011; Mohr et al., 2012).

32 While the concentration of SOA varies through the year, the extent of SOA oxidation shows
33 no variability as a function of time of year or temperature and remains within a very narrow

1 range of values. This could be explained, in part, by the geographical position of London,
2 which leads to influences from both local sources and transported air masses from all
3 directions. SOA in London forms from a variety of precursors across the year (Holmes et al.,
4 2014) where the contributions of different precursors will change significantly with season.
5 In addition, the greater photochemistry during the summer results in an increase in SOA
6 mass. However, the fraction of oxygen per molecule does not vary as the increase in locally
7 produced fresh SOA likely masks any increase in the oxidation of transported material
8 resulting in chemically similar SOA throughout the year. Whether this extends to similar
9 urban background sites in other locations remains to be determined but if so, it makes a
10 characterisation of SOA in urban environments more straightforward than may be previously
11 supposed, as the range of precursors and processes appears to lead to consistent average
12 characteristics.

13

14 **6 Pollution events in London**

15 Acute and short-term exposures to particulates have been associated with various adverse
16 health effects including cardiovascular mortality as well as exacerbating existing illnesses
17 such as pulmonary disease (Pope and Dockery, 2006 and references therein). It is therefore
18 important to investigate episodic pollution events to better understand their effects on human
19 health. During 2012, the average total NR-PM₁ concentration (\pm one standard deviation) was
20 9.91 (\pm 10.39) $\mu\text{g m}^{-3}$ in London, with slightly higher concentrations in the winter than
21 summer (Fig. 8a). Several pollution events occurred throughout the year where the
22 contributions to the high concentrations differed for each of the NR-PM₁ components
23 depending on the time of year. To determine whether emissions or atmospheric processes are
24 the controlling factor in driving such high concentration events, the contributions of the
25 different species to the top 10th percentile of the total annual concentration are assessed (Figs.
26 8a and b). Furthermore, the top 10th percentile of the winter and summer periods (Figs. 8c and
27 d, respectively) are also analysed to evaluate any seasonal changes in the dominant species
28 and sources.

29 Secondary aerosols are found to dominate throughout the year (Fig. 8b), irrespective of
30 season, although the individual contributions from SIA and SOA change between winter and
31 summer (Figs. 8c and d). High concentration events are dominated by nitrate in the winter
32 (39%), with a greater contribution from POA than SOA to the organic fraction (79% and
33 21%, respectively). Furthermore, SFOA_{mod} is the greatest component of POA (43%) and total

1 organic fraction (34%). In contrast, the high concentration events in summer are dominated
2 by organics (54%), with a significant contribution from SOA (47%), although POA is still the
3 dominant component of the organic fraction (53%). Nevertheless, the largest contribution to
4 the organic fraction is from OOA1 (42%).

5 Pollution events in the winter are therefore driven by particulate emissions, especially nitrate
6 and SFOA, whereas in the summer greater photochemistry results in higher concentrations
7 predominantly comprised of SOA. Furthermore, the average mass of the pollution events in
8 the winter is greater than that of the summer, suggesting that the limits for daily average
9 concentrations, set to improve air quality and protect human health, are more likely to be
10 exceeded in the winter than summer. Therefore, moderating sources of particulates is likely
11 to be the most effective way of reducing particulates in the winter, although this does not
12 consider the refractory sources of aerosol, such as black carbon, which contribute to the total
13 PM mass in urban areas (e.g. Liu et al., 2014).

14

15 **7 Conclusions**

16 A full calendar year of NR-PM₁ chemical composition data were acquired using a cToF-
17 AMS at an urban background site in North Kensington, London, where secondary aerosols
18 comprise approximately 71% of the total non-refractory submicron mass. Nitrate exhibited
19 strong seasonality, peaking in the spring as a result of favourable local meteorological
20 conditions and a peak in ammonia emissions. Several high nitrate concentration events
21 occurred throughout the year, which were the result of a combination of ambient conditions,
22 availability of precursors, and air mass trajectory. Contrastingly, sulphate concentrations in
23 London are predominantly influenced by regional pollution with few or no local sources and
24 ammonium concentrations are governed by the availability of precursor emissions and
25 meteorological conditions. Non-refractory chloride concentrations peak in the winter,
26 governed by the lower temperatures favouring ammonium chloride partitioning to the aerosol
27 phase.

28 The organic fraction was separated into five factors using PMF analysis: HOA, COA,
29 SFOA_{PMF}, OOA1 and OOA2_{PMF}. However, PMF was unable to account for the variance of
30 two factors across the year, resulting in the assignment of some SFOA_{PMF} mass to OOA_{PMF} as
31 indicated by comparison of the factors derived from cToF-PMF and HR-PMF during the
32 winter IOP. Based on the relationship between SFOA_{PMF} and OOA2_{PMF} from the winter at

1 the start and end of 2012, daily concentrations of SFOA_{mod} and OOA2_{mod} were calculated for
2 the year. OOA1 exhibited characteristics consistent with regional behaviour whereas
3 OOA2_{mod} exhibited a seasonal trend typical of SOA, peaking in the summer when VOC
4 emissions and photochemistry are greatest.

5 Although there is a substantial change in the concentration of SOA through the year, the
6 extent of oxidation of the SOA, as defined by the oxygen content of organic aerosol mass,
7 shows no variability as a function of time of year, air mass history, or temperature at the site.
8 This suggests that in the urban background of London the range of precursors and chemical
9 processing are insufficiently variable to yield secondary organic aerosol that has been
10 exposed to significantly different levels of chemical processing. This is surprising given the
11 variation in precursors throughout the year and the strong annual cycle in photochemical
12 activity. However, this could make characterisation of SOA in urban environments more
13 straightforward than may be previously supposed, as the range of precursors and processes
14 appears to lead to consistent average characteristics.

15 Several high concentration events occurred in London during 2012, driven by particulate
16 emissions in the winter and formation of SOA in the summer due to the greater
17 photochemistry. The limits for daily average concentrations set to improve air quality and
18 protect human health are more likely to be exceeded in the winter as the events had a greater
19 average mass than those in summer. Moderating sources of nitrate and POA is likely to be the
20 most effective way of reducing particulates in the winter, and due to the dominance of this
21 season to the annual mean, for the whole year. SFOA, COA, and HOA all make a substantial
22 contribution to the POA fraction; however SFOA, along with COA, are less well
23 characterised than HOA so their variability requires further investigation.

24

25

26 **Acknowledgements**

27 This work was supported in part by the UK Natural Environment Research Council (NERC)
28 ClearfLo project [grant ref. NE/H008136/1] and is co-ordinated by the National Centre for
29 Atmospheric Science (NCAS). Additional support for the aerosol measurements was
30 provided by the Department of Environment, Food and Rural Affairs (DEFRA). D. E. Young
31 was supported by a NERC PhD studentship [ref. NE/I528142/1]. The authors would like to
32 thank Anja Tremper at King's College London for assisting with instrument maintenance and

1 James Lee from NCAS at the University of York for logistical assistance at the North
2 Kensington supersite during the IOPs. Additional thanks to the Sion Manning School in
3 North Kensington and adjacent community centre.
4

1 **References**

- 2 Abdalmogith, S. S. and Harrison, R. M.: The use of trajectory cluster analysis to examine the
3 long-range transport of secondary inorganic aerosol in the UK, *Atmos. Environ.*, 39, 6686–
4 6695, doi:10.1016/j.atmosenv.2005.07.059, 2005.
- 5 Abdalmogith, S. S. and Harrison, R. M.: An analysis of spatial and temporal properties of
6 daily sulphate, nitrate and chloride concentrations at UK urban and rural sites, *J. Environ.*
7 *Monitor*, 8, 691–699, 2006.
- 8 Aiken, A. C., DeCarlo, P. F., Kroll, J. H., Worsnop, D. R., Huffman, J. A., Docherty, K. S.,
9 Ulbrich, I. M., Mohr, C., Kimmel, J. R., Sueper, D., Sun, Y., Zhang, Q., Trimborn, A.,
10 Northway, M., Ziemann, P. J., Canagaratna, M. R., Onasch, T. B., Alfarra, M. R., Prevot, A.
11 S. H., Dommen, J., Duplissy, J., Metzger, A., Baltensperger, U., and Jimenez, J. L.: O/C and
12 OM/OC ratios of primary, secondary, and ambient organic aerosols with high resolution
13 time-of-flight aerosol mass spectrometry, *Environ. Sci. Technol.*, 42, 4478–4485,
14 doi:10.1021/es703009q, 2008.
- 15 Allan, J. D., Jimenez, J. L., Williams, P. I., Alfarra, M. R., Bower, K. N., Jayne, J. T., Coe,
16 H., and Worsnop, D. R.: Quantitative sampling using an Aerodyne aerosol mass
17 spectrometer: 1. Techniques of data interpretation and error analysis, *J. Geophys. Res.-*
18 *Atmos.*, 108, 4090, doi:10.1029/2002JD002358s, 2003.
- 19 Allan, J. D., Williams, P. I., Morgan, W. T., Martin, C. L., Flynn, M. J., Lee, J., Nemitz, E.,
20 Phillips, G. J., Gallagher, M. W., and Coe, H.: Contributions from transport, solid fuel
21 burning and cooking to primary organic aerosols in two UK cities, *Atmos. Chem. Phys.*, 10,
22 647–668, 2010.
- 23 Ansari, A.S. and Pandis, S. N.: Response of Inorganic PM to Precursor Concentrations,
24 *Environ. Sci. Technol.*, 32, 2706-2714, 1998.
- 25 Aphekom Summary Report: Aphekom – Summary Report of the Aphekom Project 2008–
26 2011, 2011.
- 27 AQEG: Fine particulate matter (PM_{2.5}) in the United Kingdom, Report of the UK Air
28 Quality Expert Group. Prepared for: Department for Environment, Food and Rural Affairs;
29 Scottish Executive; Welsh Government; and Department of the Environment in Northern
30 Ireland, 2012.

1 Bigi, A. and Harrison, R.M.: Analysis of the air pollution climate at a central urban
2 background site, *Atmos. Environ.* 44, 2004-2012, 2010.

3 Bohnenstengel, S. I., Belcher, S. E., Aiken, A. C., Allan, J. D., Allen, G., Bacak, A., Bannan,
4 T. J., Barlow, J. F., Beddows, D. C. S., Bloss, W. J., Booth, A. M., Chemel, C., Coceal, O.,
5 Di Marco, C. F., Mavendra, D. K., Faloon, K. H., Fleming, Z., Furger, M., Geitl, J. K.,
6 Graves, R. R., Green, D. C., Grimmond, C. S. B., Halios, C., Hamilton, J. F., Harrison, R. M.,
7 Heal, M. R., Heard, D. E., Helfter, C., Herndon, S. C., Holmes, R. E., Hopkins, J. R., Jones,
8 A. M., Kelly, F. J., Kotthaus, S., Langford, B., Lee, J. D., Leigh, R. J., Lewis, A. C., Lidster,
9 R. T., Lopez-Hilfiker, F. D., McQuaid, J. B., Mohr, C., Monks, P. S., Nemitz, E., Ng, N. L.,
10 Percival, C. J., Prévôt, A. S. H., Ricketts, H. M. A., Sokhi, R., Stone, D., Thornton, J. A.,
11 Tremper, A. H., Valach, A. C., Visser, S., Whalley, L. K., Williams, L. R., Xu, L., Young, D.
12 E., and Zotter, P.: Meteorology, air quality and health in London: The ClearfLo project, *B.*
13 *Am. Meteorol. Soc.*, in press, 2014.

14 Boucher, O., Randall, D., Artaxo, P., Bretherton, C., Feingold, G., Forster, P., Kerminen, V.-
15 M., Kondo, Y., Liao, H., Lohmann, U., Rasch, P., Satheesh, S.K., Sherwood, S., Stevens, B.
16 and Zhang, X.Y., 2013: Clouds and Aerosols. In: *Climate Change 2013: The Physical*
17 *Science Basis. Contribution of Working Group I to the Fifth Assessment Report of the*
18 *Intergovernmental Panel on Climate Change* [Stocker, T.F., D. Qin, G.-K. Plattner, M.
19 Tignor, S.K. Allen, J. Boschung, A. Nauels, Y. Xia, V. Bex and P.M. Midgley (eds.)].
20 Cambridge University Press, Cambridge, United Kingdom and New York, NY, USA.

21 Bressi, M., Sciare, J., Gherzi, V., Bonnaire, N., Nicolas, J. B., Petit, J.-E., Moukhtar, S.,
22 Rosso, A., Mihalopoulos, N., and Féron, A.: A one-year comprehensive chemical
23 characterisation of fine aerosol (PM_{2.5}) at urban, suburban and rural background sites in the
24 region of Paris (France), *Atmos. Chem. Phys. Discuss.*, 12, 29391-29442, doi:10.5194/acpd-
25 12-29391-2012, 2012.

26 Canagaratna, M. R., Jayne, J. T., Jimenez, J. L., Allan, J. D., Alfarra, M. R., Zhang, Q.,
27 Onasch, T. B., Drewnick, F., Coe, H., Middlebrook, A., Delia, A. E., Williams, L. R.,
28 Trimborn, A. M., Northway, M. J., Decarlo, P. F., Kolb, C. E., Davidovits, P., and Worsnop,
29 D. R.: Chemical and microphysical characterization of ambient aerosols with the aerodyne
30 aerosol mass spectrometer, *Mass Spectrom. Rev.*, 26, 185–222, doi:10.1002/mas.20115,
31 2007.

1 Canonaco, F., Crippa, M., Slowik, J. G., Baltensperger, U., and Prévôt, A. S. H.: SoFi, an
2 Igor based interface for the efficient use of the generalized multilinear engine (ME-2) for
3 source apportionment: application to aerosol mass spectrometer data, *Atmos. Meas. Tech.*
4 *Discuss.*, 6, 6409-6443, doi:10.5194/amtd-6-6409-2013, 2013.

5 Charron, A., Harrison, R. M., and Quincey, P.: What are the sources and conditions
6 responsible for exceedences of the 24 h PM₁₀ limit value (50 µg m⁻³) at a heavily trafficked
7 London site?, *Atmos. Environ.*, 41, 1960–1975, 2007.

8 Crippa, M., DeCarlo, P. F., Slowik, J. G., Mohr, C., Heringa, M. F., Chirico, R., Poulain, L.,
9 Freutel, F., Sciare, J., Cozic, J., Di Marco, C. F., Elsasser, M., Nicolas, J. B., Marchand, N.,
10 Abidi, E., Wiedensohler, A., Drewnick, F., Schneider, J., Borrmann, S., Nemitz, E.,
11 Zimmermann, R., Jaffrezo, J.-L., Prévôt, A. S. H., and Baltensperger, U.: Wintertime aerosol
12 chemical composition and source apportionment of the organic fraction in the metropolitan
13 area of Paris, *Atmos. Chem. Phys.*, 13, 961-981, doi:10.5194/acp-13-961-2013, 2013a.

14 Crippa, M., Canonaco, F., Slowik, J. G., El Haddad, I., DeCarlo, P. F., Mohr, C.,
15 Heringa, M. F., Chirico, R., Marchand, N., Temime-Roussel, B., Abidi, E., Poulain, L.,
16 Wiedensohler, A., Baltensperger, U., and Prévôt, A. S. H.: Primary and secondary organic
17 aerosol origin by combined gas-particle phase source apportionment, *Atmos. Chem. Phys.*,
18 13, 8411-8426, doi:10.5194/acp-13-8411-2013, 2013b.

19 Cross, E. S., Slowik, J. G., Davidovits, P., Allan, J. D., Worsnop, D. R., Jayne, J. T., Lewis,
20 D. K., Canagaratna, M., and Onasch, T. B.: Laboratory and ambient particle density
21 determinations using light scattering in conjunction with aerosol mass spectrometry, *Aerosol*
22 *Sci. Tech.*, 41, 343–359, 2007.

23 Dall'Osto, M., Ovadnevaite, J., Ceburnis, D., Martin, D., Healy, R. M., O'Connor, I. P.,
24 Kourtchev, I., Sodeau, J. R., Wenger, J. C., and O'Dowd, C.: Characterization of urban
25 aerosol in Cork city (Ireland) using aerosol mass spectrometry, *Atmos. Chem. Phys.*, 13,
26 4997-5015, doi:10.5194/acp-13-4997-2013, 2013.

27 DeCarlo, P. F., Kimmel, J. R., Trimborn, A., Northway, M. J., Jayne, J. T., Aiken, A. C.,
28 Gonin, M., Fuhrer, K., Horvath, T., Docherty, K. S., Worsnop, D. R., and Jimenez, J. L.:
29 Field-deployable, high-resolution, time-of-flight aerosol mass spectrometer, *Anal. Chem.*, 78,
30 8281–8289, doi:10.1021/ac061249n, 2006.

31 DeCarlo, P. F., Dunlea, E. J., Kimmel, J. R., Aiken, A. C., Sueper, D., Crouse, J.,
32 Wennberg, P. O., Emmons, L., Shinozuka, Y., Clarke, A., Zhou, J., Tomlinson, J., Collins, D.

1 R., Knapp, D., Weinheimer, A. J., Montzka, D. D., Campos, T., and Jimenez, J. L.: Fast
2 airborne aerosol size and chemistry measurements above Mexico City and Central Mexico
3 during the MILAGRO campaign, *Atmos. Chem. Phys.*, 8, 4027–4048, doi:10.5194/acp-8-
4 4027-2008, 2008.

5 Donahue, N. M., Kroll, J. H., Pandis, S. N., and Robinson, A. L.: A two-dimensional
6 volatility basis set – Part 2: Diagnostics of organic-aerosol evolution, *Atmos. Chem. Phys.*,
7 12, 615–634, doi:10.5194/acp-12-615-2012, 2012.

8 Drewnick, F., Hings, S. S., Decarlo, P. F., Jayne, J. T., Gonin, M., Fuhrer, K., Weimer, S.,
9 Jimenez, J. L., Demerjian, K. L., Borrmann, S., and Worsnop, D. R.: A new time-of-flight
10 aerosol mass spectrometer (TOF-AMS) - Instrument description and first field deployment,
11 *Aerosol Sci. Tech.*, 39, 637–658, doi:10.1080/02786820500182040, 2005.

12 EEA: The European environment — state and outlook 2010: synthesis. European
13 Environment Agency, Copenhagen, 2010.

14 European Union: Directive 2008/50/EC of the European parliament and of the council of 21
15 May 2008 on ambient air quality and cleaner air for Europe, *Official Journal of the European*
16 *Union*, L152, 2008.

17 El Haddad, I., Marchand, N., D’Anna, B., Jaffrezo, J.-L., and Wortham, H.: Functional
18 group composition of organic aerosol from combustion emissions and secondary processes at
19 two contrasted urban environments, *Atmos. Environ.*, 75, 308–320,
20 doi:10.1016/j.atmosenv.2013.04.019, 2013.

21 Freutel, F., Schneider, J., Drewnick, F., von der Weiden-Reinmüller, S.-L., Crippa, M.,
22 Prévôt, A. S. H., Baltensperger, U., Poulain, L., Wiedensohler, A., Sciare, J., Sarda-
23 Estève, R., Burkhardt, J. F., Eckhardt, S., Stohl, A., Gros, V., Colomb, A., Michoud, V.,
24 Doussin, J. F., Borbon, A., Haeffelin, M., Morille, Y., Beekmann, M., and Borrmann, S.:
25 Aerosol particle measurements at three stationary sites in the megacity of Paris during
26 summer 2009: meteorology and air mass origin dominate aerosol particle composition and
27 size distribution, *Atmos. Chem. Phys.*, 13, 933-959, doi:10.5194/acp-13-933-2013, 2013.

28 Goldstein, A.H., and Galbally, I.E.: Known and unexplored organic constituents in the
29 Earth’s atmosphere. *Environ. Sci. Technol.*, 41, 1515–1521, 2007.

30 Harrison, R. M., Dall’Osto, M., Beddows, D. C. S., Thorpe, A. J., Bloss, W. J., Allan, J. D.,
31 Coe, H., Dorsey, J. R., Gallagher, M., Martin, C., Whitehead, J., Williams, P. I., Jones, R. L.,

1 Langridge, J. M., Benton, A. K., Ball, S. M., Langford, B., Hewitt, C. N., Davison, B.,
2 Martin, D., Petersson, K. F., Henshaw, S. J., White, I. R., Shallcross, D. E., Barlow, J. F.,
3 Dunbar, T., Davies, F., Nemitz, E., Phillips, G. J., Helfter, C., Di Marco, C. F., and Smith, S.:
4 Atmospheric chemistry and physics in the atmosphere of a developed megacity (London): an
5 overview of the REPARTEE experiment and its conclusions, *Atmos. Chem. Phys.*, 12, 3065-
6 3114, doi:10.5194/acp-12-3065-2012, 2012.

7 Harrison, R. M. and Yin, J.: Sources and processes affecting carbonaceous aerosol in central
8 England, *Atmos. Environ.*, 42, 1413-1423, 2008.

9 Huang, R.-J., Zhang, Y., Bozzetti, C., Ho, K.-F., Cao, J.-J., Han, Y., Daellenbach, K. R.,
10 Slowik, J. G., Platt, S. M., Canonaco, F., Zotter, P., Wolf, R., Pieber, S. M., Bruns, E. A.,
11 Crippa, M., Ciarelli, G., Piazzalunga, A., Schwikowski, M., Abbaszade, G., Schnelle-Kreis,
12 J., Zimmerman, R., An, Z., Szidat, S., Baltensperger, R., El Haddad, I. and Prévôt, A. S. H.:
13 High secondary aerosol contribution to particulate pollution during haze events in China,
14 *Nature*, 514, 218-222, doi:10.1038/nature13774, 2014.

15 Heald, C. L., Kroll, J. H., Jimenez, J. L., Docherty, K. S., DeCarlo, P. F., Aiken, A. C., Chen,
16 Q., Martin, S. T., Farmer, D. K., and Artaxo, P.: A simplified description of the evolution of
17 organic aerosol composition in the atmosphere, *Geophys. Res. Lett.*, 37, L08 803,
18 doi:10.1029/2010GL042737, 2010.

19 Holmes, R. E., Hopkins, J. R., Lidster, R. T., Lee, J. D., Evans, M. J., Lewis, A. C., and
20 Hamilton, J. F.: Diesel-related hydrocarbons dominate reactive carbon in modern megacity
21 atmospheres, in preparation, 2014.

22 Huffman, J. A., Ziemann, P. J., Jayne, J. T., Worsnop, D. R., and Jimenez, J. L.:
23 Development and Characterization of a Fast-Stepping/Scanning Thermodenuder for
24 Chemically-Resolved Aerosol Volatility Measurements, *Aerosol Sci. Technol.*, 42, 395–407,
25 2008.

26 Jayne, J. T., Leard, D. C., Zhang, X. F., Davidovits, P., Smith, K. A., Kolb, C. E., and
27 Worsnop, D. R.: Development of an aerosol mass spectrometer for size and composition
28 analysis of submicron particles, *Aerosol Sci. Tech.*, 33, 49–70,
29 doi:10.1080/027868200410840, 2000.

30 Jimenez, J. L., Canagaratna, M. R., Donahue, N. M., Prevot, A. S. H., Zhang, Q., Kroll, J. H.,
31 Decarlo, P. F., Allan, J. D., Coe, H., Ng, N. L., Aiken, A. C., Docherty, K. S., Ulbrich, I. M.,

1 Grieshop, A. P., Robinson, A. L., Duplissy, J., Smith, J. D., Wilson, K. R., Lanz, V. A.,
2 Hueglin, C., Sun, Y. L., Tian, J., Laaksonen, A., Raatikainen, T., Rautiainen, J., Vaattovaara,
3 P., Ehn, M., Kulmala, M., Tomlinson, J. M., Collins, D. R., Cubison, M. J., E., Dunlea, E. J.,
4 Huffman, J. A., Onasch, T. B., Alfarra, M. R., Williams, P. I., Bower, K. N., Kondo, Y.,
5 Schneider, J., Drewnick, F., Borrmann, S., Weimer, S., Demerjian, K. L., Salcedo, D.,
6 Cottrell, L., Griffin, R., Takami, A., Miyoshi, T., Hatakeyama, S., Shimono, A., Sun, J. Y.,
7 Zhang, Y. M., Dzepina, K., Kimmel, J. R., Sueper, D., Jayne, J. T., Herndon, S. C.,
8 Trimborn, A. M., Williams, L. R., Wood, E. C., Middlebrook, A. M., Kolb, C. E.,
9 Baltensperger, U., and Worsnop, D. R.: Evolution of Organic Aerosols in the Atmosphere,
10 *Science*, 326, 1525–1529, doi:10.1126/science.1180353, 2009.

11 Kroll, J. H., Donahue, N. M., Jimenez, J. L., Kessler, S. H., Canagaratna, M. R., Wilson, K.
12 R., Altieri, K. E., Mazzoleni, L. R., Wozniak, A. S., Bluhm, H., Mysak, E. R., Smith, J. D.,
13 Kolb, C. E., and Worsnop, D. R.: Carbon Oxidation State as a Metric for Describing the
14 Chemistry of Atmospheric Organic Aerosol, *Nature Chem.*, 3, 133–139,
15 doi:10.1038/NCHEM.948, 2011.

16 Lanz, V. A., Alfarra, M. R., Baltensperger, U., Buchmann, B., Hueglin, C., and
17 Prévôt, A. S. H.: Source apportionment of submicron organic aerosols at an urban site by
18 factor analytical modelling of aerosol mass spectra, *Atmos. Chem. Phys.*, 7, 1503–1522,
19 doi:10.5194/acp-7-1503-2007, 2007.

20 Lanz, V. A., Alfarra, M. R., Baltensperger, U., Buchmann, B., Hueglin, C., Szidat, S.,
21 Wehrli, M. N., Wacker, L., Weimer, S., Caseiro, A., Puxbaum, H., and Prévôt, A. S. H.:
22 Source attribution of submicron organic aerosols during wintertime inversions by advanced
23 factor analysis of aerosol mass spectra, *Environ. Sci. Technol.*, 42, 214–220,
24 doi:10.1021/es0707207s, 2008.

25 Liu, D., Allan, J. D., Young, D. E., Coe, H., Beddows, D., Fleming, Z. L., Flynn, M. J.,
26 Gallagher, M. W., Harrison, R. M., Lee, J., Prévôt, A. S. H., Taylor, J. W., Yin, J., Williams,
27 P. I., and Zotter, P.: Size distribution, mixing state and source apportionments of black carbon
28 aerosols in London during winter time, *Atmos. Chem. Phys. Discuss.*, 14, 16291–16349,
29 doi:10.5194/acpd-14-16291-2014, 2014.

30 Martin, C. L., Allan, J. D., Crosier, J., Choularton, T. W., Coe, H., and Gallagher, M. W.:
31 Seasonal variation of fine particulate composition in the centre of a UK city, *Atmos.*
32 *Environ.*, 45, 4379–4389, 10.1016/j.atmosenv.2011.05.050, 2011.

1 Megaritis, A. G., Fountoukis, C., Charalampidis, P. E., Pilinis, C., and Pandis, S. N.:
2 Response of fine particulate matter concentrations to changes of emissions and temperature in
3 Europe, *Atmos. Chem. Phys.*, 13, 3423-3443, doi:10.5194/acp-13-3423-2013, 2013.

4 Middlebrook, A. M., Bahreini, R., Jimenez, J. L., and Canagaratna, M. R.: Evaluation of
5 composition-dependent collection efficiencies for the Aerodyne aerosol mass spectrometer
6 using field data, *Aerosol. Sci. Tech.*, 46, 258–271, doi:10.1080/02786826.2011.620041,
7 2012.

8 Mohr, C., Huffman, J. A., Cubison, M. J., Aiken, A. C., Docherty, K. S., Kimmel, J. R.,
9 Ulbrich, I. M., Hannigan, M., Garcia, J., and Jimenez, J. L.: Characterization of Primary
10 Organic Aerosol Emissions from Meat Cooking, Trash Burning, and Motor Vehicles with
11 High-Resolution Aerosol Mass Spectrometry and Comparison with Ambient and Chamber
12 Observations, *Environ. Sci. Technol.*, 43, 2443–2449, doi:10.1021/es8011518, 2009.

13 Mohr, C., DeCarlo, P. F., Heringa, M. F., Chirico, R., Slowik, J. G., Richter, R., Reche, C.,
14 Alastuey, A., Querol, X., Seco, R., Peñuelas, J., Jiménez, J. L., Crippa, M., Zimmermann, R.,
15 Baltensperger, U., and Prévôt, A. S. H.: Identification and quantification of organic aerosol
16 from cooking and other sources in Barcelona using aerosol mass spectrometer data, *Atmos.*
17 *Chem. Phys.*, 12, 1649-1665, doi:10.5194/acp-12-1649-2012, 2012.

18 Monks, P. S., Granier, C., Fuzzi, S., Stohl, A., Williams, M. L., Akimoto, H., Amann, M.,
19 Baklanov, A., Baltensperger, U., Bey, I., Blake, N., Blake, R. S., Carslaw, K. S., Cooper, O.
20 R., Dentener, F. J., Fowler, D., Fragkou, E., Frost, G. J., Generoso, S., Ginoux, P., Grewe, V.,
21 Guenther, A., Hansson, H. C., Henne, S., Hjorth, J., Hofzumahaus, A., Huntrieser, H.,
22 Isaksen, I. S. A., Jenkin, M. E., Kaiser, J., Kanakidou, M., Klimont, Z., Kulmala, M., Laj, P.,
23 Lawrence, M. G., Lee, J. D., Liousse, C., Maione, M., McFiggans, G. B., Metzger, A.,
24 Mieville, A., Moussiopoulos, N., Orlando, J. J., O'Dowd, C. D., Palmer, P. I., Parrish, D. D.,
25 Petzold, A., Platt, U., Pöschl, U., Prévôt, A. S. H., Reeves, C. E., Reimann, S., Rudich, Y.,
26 Sellegri, K., Steinbrecher, R., Simpson, D., ten Brink, H., Theloke, J., van Der Werf, G. R.,
27 Vautard, R., Vestreng, V., Vlachokostas, C., and von Glasow, R.: Atmospheric composition
28 change – global and regional air quality, *Atmos. Environ.*, 43, 5268–5350, doi:
29 10.1016/j.atmosenv.2009.08.021, 2009.

30 Morgan, W. T., Allan, J. D., Bower, K. N., Capes, G., Crosier, J., Williams, P. I., and
31 Coe, H.: Vertical distribution of sub-micron aerosol chemical composition from North-

1 Western Europe and the North-East Atlantic, *Atmos. Chem. Phys.*, 9, 5389-5401,
2 doi:10.5194/acp-9-5389-2009, 2009.

3 Morgan, W. T., Allan, J. D., Bower, K. N., Highwood, E. J., Liu, D., McMeeking, G. R.,
4 Northway, M. J., Williams, P. I., Krejci, R., and Coe, H.: Airborne measurements of the
5 spatial distribution of aerosol chemical composition across Europe and evolution of the
6 organic fraction, *Atmos. Chem. Phys.*, 10, 4065-4083, doi:10.5194/acp-10-4065-2010, 2010.

7 National atmospheric emissions inventory (NAEI): <http://naei.defra.gov.uk/> (last access: 24
8 December 2013), 2013.

9 Ng, N. L., Canagaratna, M. R., Zhang, Q., Jimenez, J. L., Tian, J., Ulbrich, I. M., Kroll, J. H.,
10 Docherty, K. S., Chhabra, P. S., Bahreini, R., Murphy, S. M., Seinfeld, J. H., Hildebrandt, L.,
11 Donahue, N. M., DeCarlo, P. F., Lanz, V. A., Prévôt, A. S. H., Dinar, E., Rudich, Y., and
12 Worsnop, D. R.: Organic aerosol components observed in Northern Hemispheric datasets
13 from Aerosol Mass Spectrometry, *Atmos. Chem. Phys.*, 10, 4625-4641, doi:10.5194/acp-10-
14 4625-2010, 2010.

15 Ng, N. L., Herndon, S. C., Trimborn, A., Canagaratna, M. R., Croteau, P., Onasch, T. M.,
16 Sueper, D., and Worsnop, D. R.: An Aerosol Chemical Speciation Monitor (ACSM) for
17 routine monitoring of atmospheric aerosol composition, *Aerosol Sci. Technol.*, 45, 770–784,
18 2011a.

19 Ng, N. L., Canagaratna, M. R., Jimenez, J. L., Chhabra, P. S., Seinfeld, J. H., and
20 Worsnop, D. R.: Changes in organic aerosol composition with aging inferred from aerosol
21 mass spectra, *Atmos. Chem. Phys.*, 11, 6465-6474, doi:10.5194/acp-11-6465-2011, 2011b.

22 Oberdörster, G., Oberdörster, E., and Oberdörster, J.: Nanotoxicology: An emerging
23 discipline evolving from studies of ultrafine particles, *Environ. Health Persp.*, 113, 823–839,
24 2005.

25 Paatero, P. and Tapper, U.: Positive matrix factorization – a nonnegative factor model with
26 optimal utilization of error-estimates of data values, *Environmetrics*, 5, 111–126, 1994.

27 Pope, C. A. III and Dockery, D. W.: Health Effects of Fine Particulate Air Pollution: Lines
28 that Connect, *J. Air Waste Manage.*, 56, 709-742, DOI: 10.1080/10473289.2006.10464485,
29 2006.

30 Pöschl, U.: Atmospheric aerosols: composition, transformation, climate and health effects,
31 *Angew. Chem. Int. Ed.*, 44, 7520– 7540, 2005.

1 Schaap, M., van Loon, M., ten Brink, H. M., Dentener, F. J., and Builtjes, P. J. H.: Secondary
2 inorganic aerosol simulations for Europe with special attention to nitrate, *Atmos. Chem.
3 Phys.*, 4, 857-874, doi:10.5194/acp-4-857-2004, 2004.

4 Seinfeld, J. H. and Pandis, S. N.: *Atmospheric chemistry and physics: from air pollution to
5 climate change*, Second Edition, John Wiley & Sons, New York, 2006.

6 Stelson, A. and Seinfeld, J.: Relative humidity and temperature dependence of the ammonium
7 nitrate dissociation constant, *Atmos. Environ.*, 16, 983–992,
8 doi:10.1016/j.atmosenv.2007.10.063, 1982.

9 Sueper, D.: ToF-AMS High Resolution Analysis Software – Pika, online available at:
10 <http://cires.colorado.edu/jimenez-group/ToFAMSResources/ToFSoftware/index.html>, 2008.

11 Sun, Y.-L., Zhang, Q., Schwab, J. J., Demerjian, K. L., Chen, W.-N., Bae, M.-S., Hung, H.-
12 M., Hogrefe, O., Frank, B., Rattigan, O. V., and Lin, Y.-C.: Characterization of the sources
13 and processes of organic and inorganic aerosols in New York city with a high-resolution
14 time-of-flight aerosol mass spectrometer, *Atmos. Chem. Phys.*, 11, 1581-1602,
15 doi:10.5194/acp-11-1581-2011, 2011.

16 Sun, Y. L., Wang, Z. F., Fu, P. Q., Yang, T., Jiang, Q., Dong, H. B., Li, J., and Jia, J. J.:
17 Aerosol composition, sources and processes during wintertime in Beijing, China, *Atmos.
18 Chem. Phys.*, 13, 4577-4592, doi:10.5194/acp-13-4577-2013, 2013.

19 Sutton, M. A., Dragosits, U. Tang, Y. S., and Fowler, D.: Ammonia emissions from non-
20 agricultural sources in the UK, *Atmos. Environ.*, 34, 855-869, 2000.

21 Takegawa, N., Miyakawa, T., Kondo, Y., Jimenez, J. L., Zhang, Q., Worsnop, D. R., and
22 Fukuda, M.: Seasonal and diurnal variations of submicron organic aerosol in Tokyo observed
23 using the Aerodyne aerosol mass spectrometer, *J. Geophys. Res.*, 111, D11206,
24 doi:10.1029/2005JD006515, 2006.

25 Ulbrich, I. M., Canagaratna, M. R., Zhang, Q., Worsnop, D. R., and Jimenez, J. L.:
26 Interpretation of organic components from Positive Matrix Factorization of aerosol mass
27 spectrometric data, *Atmos. Chem. Phys.*, 9, 2891–2918, doi:10.5194/acp-9-2891-2918, 2009.

28 Wagener, S., Langner, M., Hansen, U., Moriske, H. J. and Endlicher, W. R.: Spatial and
29 seasonal variations of biogenic tracer compounds in ambient PM₁₀ and PM₁ samples in
30 Berlin, Germany, *Atmos. Environ.*, 47, 33-42, 2012.

1 Watson, J. G.: Visibility: Science and Regulation, *J. Air Waste Manage.*, 52, 628-713, DOI:
2 10.1080/10473289.2002.10470813, 2002.

3 WHO. Air Quality Guidelines. Global update 2005. Particulate matter, ozone, nitrogen
4 dioxide and sulphur dioxide. World Health Organization European Office. Copenhagen,
5 2005.

6 Yin, J., Harrison, R. M., Chen, Q., Rutter, A. and Schauer, J. J.: Source apportionment of
7 fine particles at urban background and rural sites in the UK Atmosphere, *Atmos. Environ.*,
8 44, 841-851, 2010.

9 Zhang, Q., Jimenez, J. L., Canagaratna, M. R., Allan, J. D., Coe, H., Ulbrich, I., Alfarra, M.
10 R., Takami, A., Middlebrook, A. M., Sun, Y. L., Dzepina, K., Dunlea, E. J., Docherty, K. S.,
11 Decarlo, P. F., Salcedo, D., Onasch, T., Jayne, J. T., Miyoshi, T., Shimo, A., Hatakeyama,
12 S., Takegawa, N., Kondo, Y., Schneider, J., Drewnick, F., Borrmann, S., Weimer, S.,
13 Demerjian, K. L., Williams, P., Bower, K. N., Bahreini, R., Cottrell, L., Griffin, R. J.,
14 Rautiainen, J., Sun, J. Y., Zhang, Y. M., and Worsnop, D. R.: Ubiquity and dominance of
15 oxygenated species in organic aerosols in anthropogenically-influenced Northern Hemisphere
16 midlatitudes, *Geophysical Research Letters*, 34, L13 801, doi:10.1029/2007GL029979, 2007.

1 Table 1. Average annual sulphate concentrations (in $\mu\text{g m}^{-3}$) from two UK locations
 2 measured between 2001 and 2012 as part of the AURN and Particulates networks. London
 3 North Kensington is an urban background monitoring site and Harwell is a rural background
 4 monitoring site.

Year	Location	
	London North Kensington	Harwell
2012	1.39 ^a , 1.21 ^{b,*}	-
2011	2.2 ^b	-
2010	2.3 ^c	1.6 ^c
2009	1.7 ^c	1.3 ^c
2008	2.6 ^c	2.4 ^c
2007	2.8 ^c	2.4 ^c
2006	3.5 ^c	3 ^c
2005	3 ^c	2.4 ^c
2004	3 ^c	2.3 ^c
2003	2.6 ^c	2.4 ^c
2002	3.1 ^c	2.3 ^c
2001	3.1 ^c	2.1 ^c

5 ^aAMS (PM₁) , ClearfLo, this study.

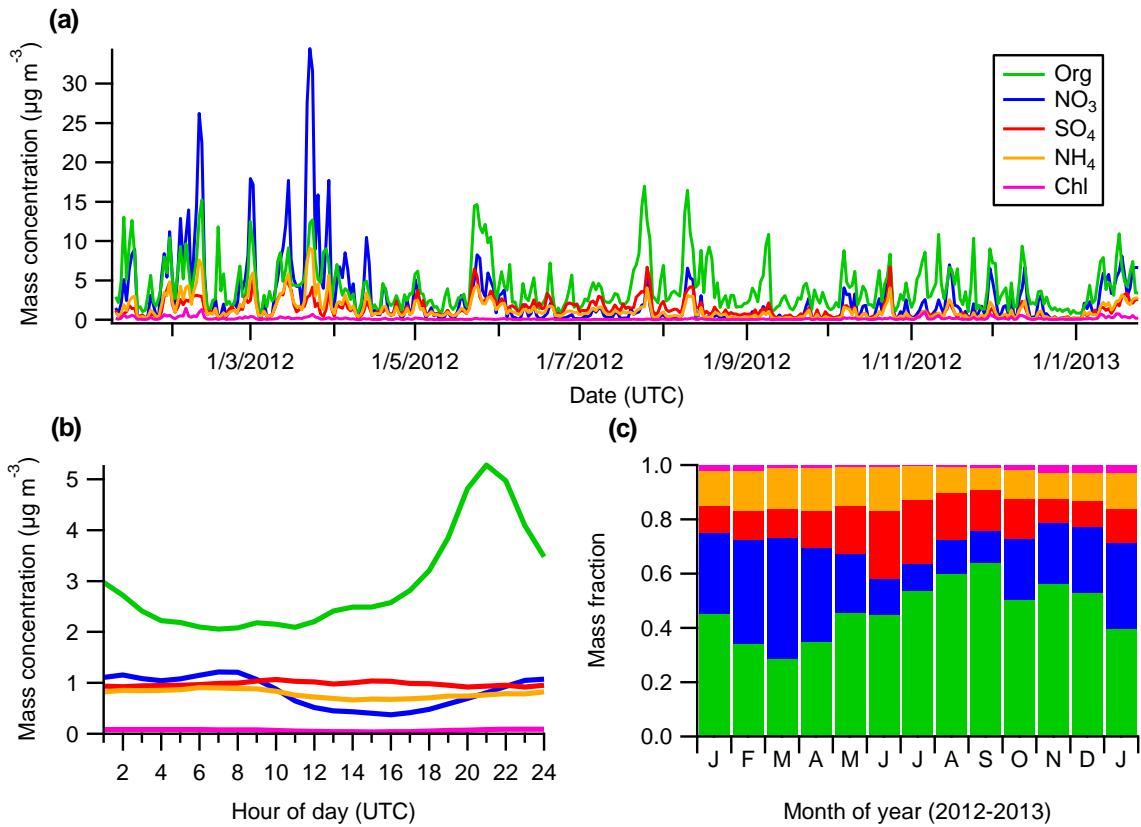
6 ^bURG 9000B Ambient Ion Monitor (AIM) (PM₁₀), KCL (Courtesy of Dr. D. Green).

7 ^cThermo Scientific Partisol 2025 ion chromatography (PM₁₀), KCL (Courtesy of Dr. D.
 8 Green).

9 *Calculated non-sea salt sulphate.

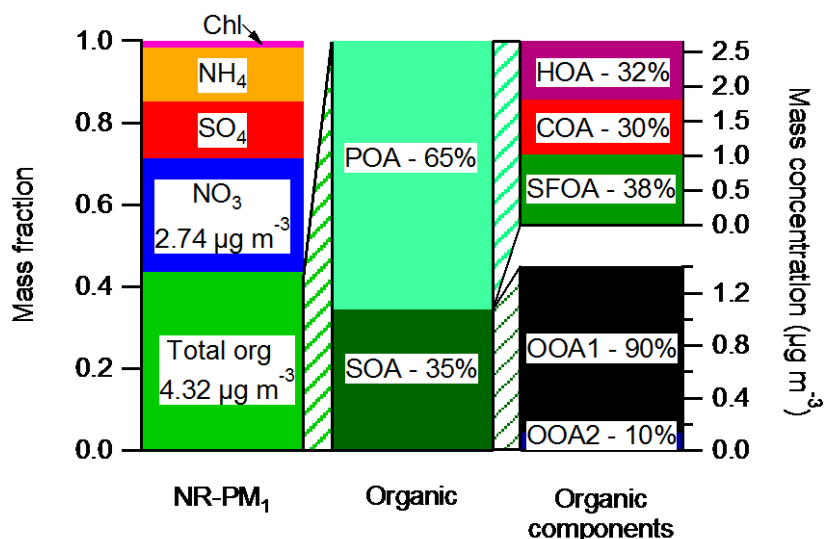
- 1 Table 2. Time series comparison of the PMF factors from the cToF-AMS and HR-ToF-AMS
- 2 for the winter IOP.

cToF-PMF factor	HR-PMF factor	Slope	Pearson's r
HOA	HOA	0.95	0.90
COA	COA	0.58	0.89
SFOA _{PMF}	SFOA1	0.80	0.87
SFOA _{PMF}	SFOA2	0.85	0.72
SFOA _{PMF}	Combined SFOA	0.52	0.90
OOA2 _{PMF}	OOA	0.12	0.16
OOA1	OOA	0.90	0.91
OOA2 _{PMF} + OOA1	OOA	1.02	0.69
SFOA _{PMF} + OOA2 _{PMF}	Combined SFOA	0.93	0.89

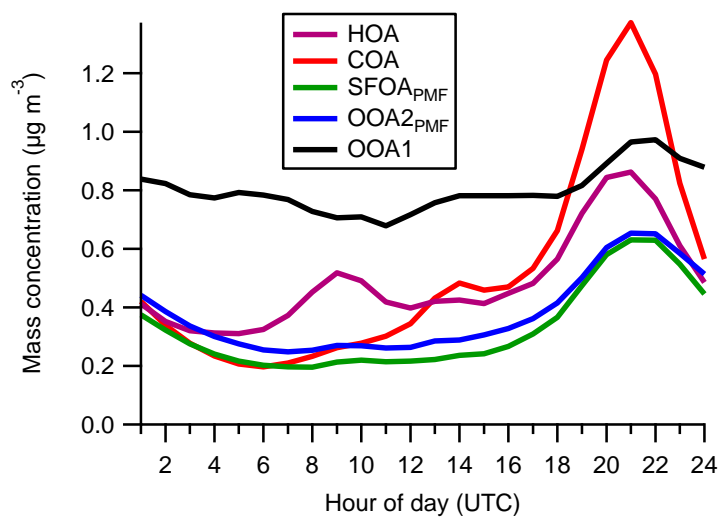


1

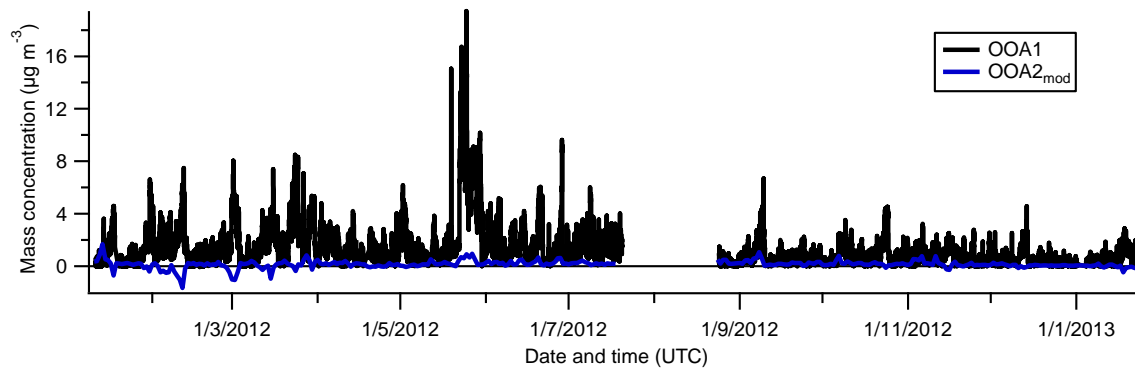
2 Figure 1. (a) Daily averaged time series of all NR-PM₁ species. (b) Median diurnal profiles of
 3 all NR-PM₁ species. (c) Average monthly fractional contribution of all species to total PM₁.
 4 The months are grouped as seasons: January 2012, February, December, and January 2013
 5 are in winter; March, April, and May are in spring; June, July, and August are in summer;
 6 September, October, and November are in autumn.



1
2 Figure 2. Left: average annual fractional contribution of all species to total NR-PM₁. The
3 average annual PM₁ concentrations of SO₄, NH₄, and Chl were 1.39, 1.30, and 0.15 $\mu\text{g m}^{-3}$,
4 respectively. Middle: Expansion of the organic fraction into its primary and secondary
5 components following PMF analysis. Right top: Expansion of the POA fraction into its three
6 components. Right bottom: Magnification of the SOA fraction showing its two subtypes.
7 SFOA and OOA2 refer to SFOA_{mod} and OOA2_{mod}, respectively. See text in Sect. 4.4 for
8 more details. Note that the organic data plotted in the middle and right bars do not include a
9 period from the summer as discussed in Sect. 4.1 as well as Sects. 4.1 and 4.2 in the
10 Supplement.

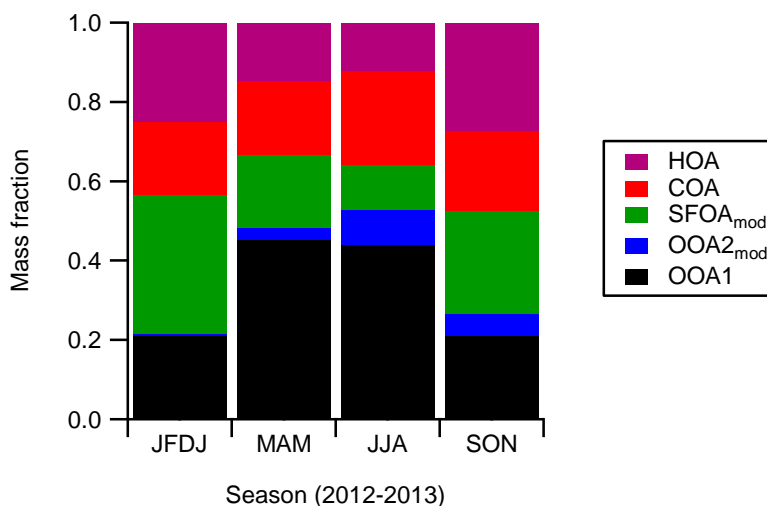


1
 2 Figure 3. Median diurnal profiles for each of the five PMF factors. Note that these data do not
 3 include a period from the summer (see Sect. 4.1).



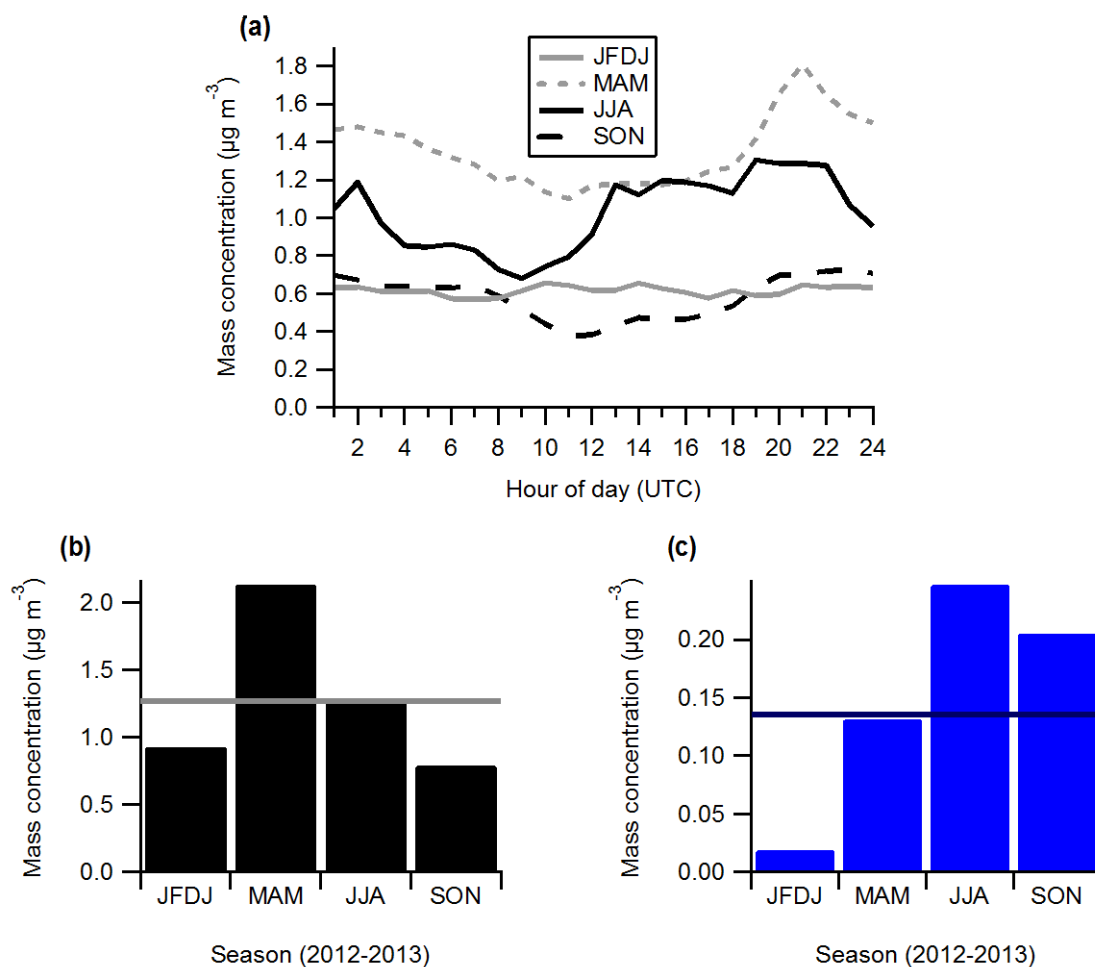
1

2 Figure 4. Time series of OOA1 and OOA2_{mod}, where OOA2_{mod} is the daily average.



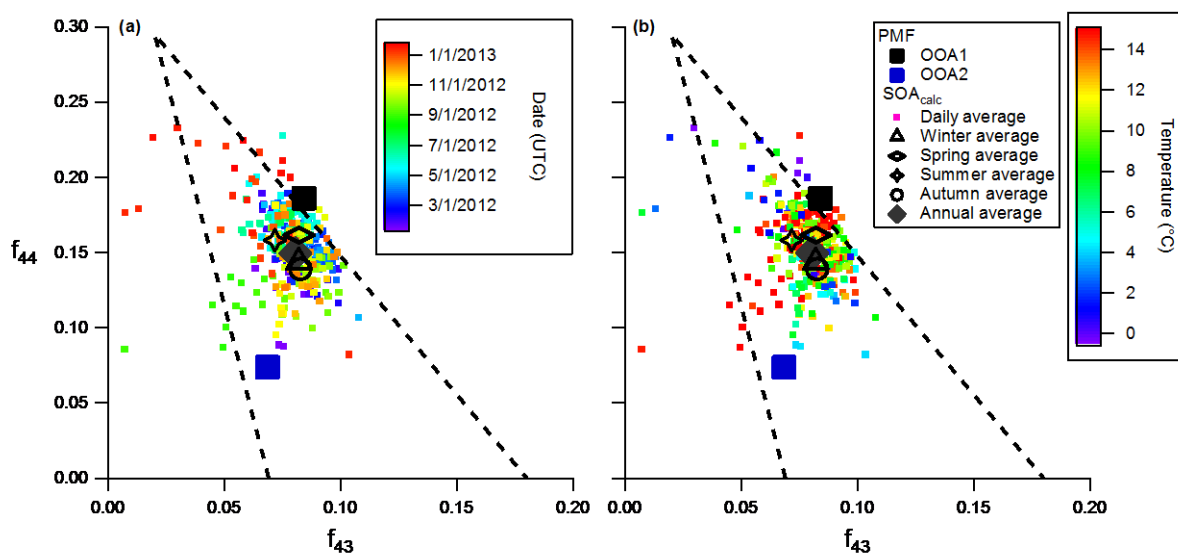
1

2 Figure 5. Seasonal fractional contributions of the PMF factors to total OA mass, with revised
 3 masses (see Section 4.4). As discussed in Sect. 4.1, a period from the summer is not included
 4 in these data.



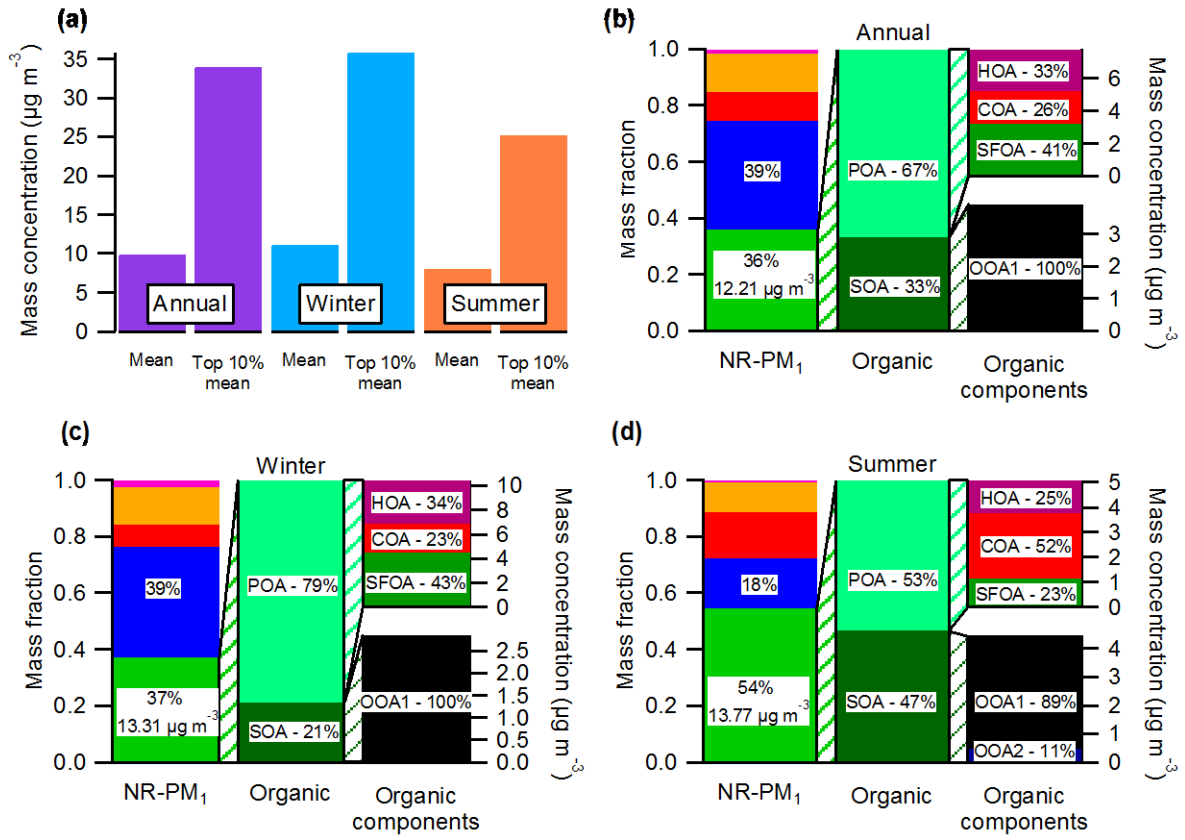
1

2 Figure 6. (a) OOA1 seasonal median diurnal profiles. (b) Average seasonal concentration of
 3 OOA1, with the annual average denoted by the thick horizontal line. (c) Average seasonal
 4 concentration of OOA2_{mod}, with the annual average denoted by the thick horizontal line, both
 5 estimated in Sect. 4.4. Note that these data do not include the summer period (see Sect. 4.1).

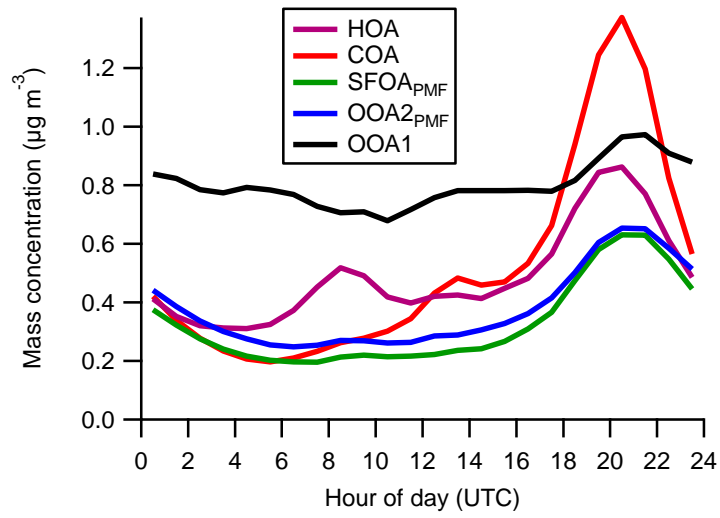


1

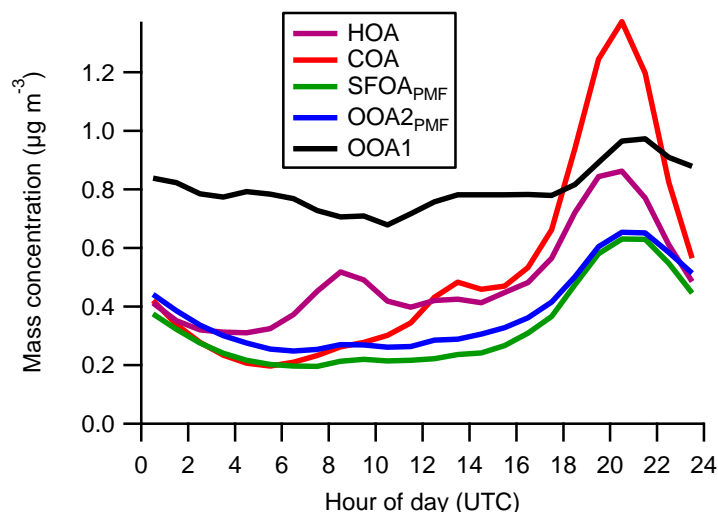
2 Figure 7. Daily averaged SOA within f_{44} vs. f_{43} space coloured by time (a) and temperature
 3 (b) where f_{44} and f_{43} refer to m/z 44:SOA_{calc} and m/z 43:SOA_{calc}, respectively. See text for
 4 more details. Daily averaged temperatures ranged from -0.5 to 26°C although are only
 5 coloured up to a maximum of 15°C here for clarity. Average annual and seasonal f_{44}/f_{43}
 6 values for SOA are denoted by the text. OOA1, OOA2 PMF factors are also plotted. The
 7 outline of the triangle as defined by Ng et al. (2010) is shown by the dashed black lines. Note
 8 that the organic data do not include the summer period (see Sect. 4.1)..



1



2



1

2 Figure 8. (a) Mean concentrations of the full calendar year (2012-2013), winter, and summer
 3 months. The average concentration of the top 10th percentile for the year as well as the top
 4 10th percentile in the winter and summer are also shown. (b) Average fractional contributions
 5 of all species to the top 10th percentile for the year, with an expansion of the organic fraction
 6 into each of its primary and secondary components. (c) Average fractional contributions of all
 7 species to the top 10th percentile in the winter, with an expansion of the organic fraction into
 8 each of its primary and secondary components. (d) Average fractional contributions of all
 9 species to the top 10th percentile in the summer, with an expansion of the organic fraction into
 10 each of its primary and secondary components. In all figures, SFOA and OOA2 refer to
 11 SFOA_{mod} and OOA2_{mod} respectively. Note that the PMF data (middle and right bars) do not
 12 include the summer period as detailed in Sect. 4.1 as well as Sects. 4.1. and 4.2 in the
 13 Supplement.

14